CAMBRIDGE UNIVERSITY PRESS

RESEARCH ARTICLE

Anticontinuous limit of discrete Landau-de Gennes theory

Panayotis Panayotaros and Guillermo Reyes Valencia

Departamento de Matematicas y Mecanica, IIMAS, Universidad Nacional Autonoma de Mexico, Mexico City, Mexico Corresponding author: Panayotis Panayotaros; Email: panos@aries.iimas.unam.mx

Keywords: bifurcation equation; discrete Landau-de Gennes equations; normal hyperbolicity

MSC Codes: Primary 6A15; Secondary 37D05; 37D10; 37C81

(Received 25 February 2025; revised 18 July 2025; accepted 22 September 2025)

Abstract

We study discretized Landau–de Gennes gradient dynamics of finite lattices and graphs in the small intersite coupling regime ("anticontinuous limit"). We consider the case of 3×3 Q-tensor systems and extend recent results on small coupling intersite equilibria to the case of geometries without boundaries. We show that the equation for Landau–de Gennes equilibria is reduced to an SO(3)-equivariant equation on submanifolds that are diffeomorphic to products of projective planes and are parametrized by uniaxial Q-tensors. The gradient flow of the Landau–de Gennes energy has a normally hyperbolic invariant attracting submanifold that is also parametrized by uniaxial Q-tensors. We also present numerical studies of the Landau–de Gennes gradient flow in open and periodic chain geometries. We see a rapid approach to a near-uniaxial state at each site, as expected by the theory, and a much slower decay to an equilibrium configuration. The long time scale is several orders of magnitudes slower, and can depend on the size of the lattice and the initial condition. In the case of the circle we see evidence for two stable equilibria that are discrete analogues of curves belonging to the two homotopy classes of the projective plane. Evidence of bistability is also seen numerically in the open chain geometry.

1. Introduction

We study the dynamics of a discretized Landau–de Gennes energy functional for 3×3 *Q*-tensors in the regime of small intersite coupling, the "anticontinuous limit" regime. Of special interest are static configurations, their stability, and their relation to equilibria of discrete Oseen–Frank energy functionals that involve a director field. The two discretized functionals are defined in finite graphs and we consider one-elastic-constant models [1, 14, 21, 28, 32].

The Oseen–Frank and Landau–de Gennes continuum theories are commonly used models for nematic liquid crystals [9, 13]. The Landau–de Gennes theory can be thought of as a generalization of the Oseen–Frank theory that includes biaxiality, spatial variations of the order parameter, and more general singular-like structures [9, 32]. Our study is partially motivated by results of Majumdar and Zarnescu [21] for 3–dimensional domains and 3×3 *Q*-tensors showing that, as the coupling constant vanishes, the minimizers of the Landau–de Gennes energy converge to Oseen–Frank minimizers. The convergence is in $W^{1,2}(D)$, $D \subset \mathbb{R}^3$ the domain, and is uniform away from the vicinity of singularities of the Oseen–Frank minimizers.

In [25] vanishing coupling constant equilibria were studied in a simpler discrete and finite setting using a combination of implicit function theorem and symmetry arguments. Similar ideas were used in proofs of existence of small intersite "breather solutions" of discrete nonlinear Schrödinger (DNLS) equations [27, 29, 30]. The strategy originates in [2, 19] and has also been applied to equilibria of

[©] The Author(s), 2025. Published by Cambridge University Press. This is an Open Access article, distributed under the terms of the Creative Commons Attribution licence (http://creativecommons.org/licenses/by/4.0), which permits unrestricted re-use, distribution and reproduction, provided the original article is properly cited.

2

discrete nonlinear parabolic equations [7]. In [25] the liquid crystal problem is also simplified by considering 2×2 *Q*-tensors. The generalization of the discrete theory to the 3×3 *Q*-tensor case requires a more systematic use of the symmetries of the decoupled problem [26], i.e. some theory of Lie group actions, see e.g. [23]. The computations used in the proof also imply that the gradient flow of the discrete Landau–de Gennes energy has a normally hyperbolic attractor, a manifold that is parametrized by the uniaxial *Q*-tensors and is diffeomorphic to a product of projective planes [25, 26]. The theory is likely relevant to other multicomponent parabolic systems with onsite nonlinearities that are invariant under Lie group actions.

The first part of the paper states and shows necessary and sufficient conditions for the continuation of equilibria of the decoupled Landau–de Gennes discrete theory in lattices and graphs without boundary, see Propositions 2.3, 2.4. The results are based on the reduction to equations on submanifolds parametrized by uniaxial Q-tensors, see Lemma 3.11. The reduction step is shown as in the case with boundary [26]. In the case without boundary the reduced equation has an additional equivariance under the diagonal adjoint action of SO(3) on products of projective planes, see Lemma 3.12, and equilibria belong to submanifolds. In Proposition 3.13, we classify the isotropy subgroups of this action, this is a first step towards classifying these manifolds. Generically, the isotropy subgroup is trivial, however nontrivial finite subgroups are also possible.

In the second part of the paper, we show results from numerical integrations of the gradient flow of the Landau—de Gennes functional in open and periodic chains, these are the simplest geometries where we expect to see multiple attracting equilibria related to the topology of the domain and the target space (projective plane). Integrating the gradient flow we see a rapid approach to configurations where the *Q*-tensor is near uniaxial at all sites and then a much slower evolution to the equilibrium. These observations are consistent with the existence of the normally hyperbolic attractor parametrized by the uniaxial *Q*-tensors. The time scale of the slower evolution is several orders of magnitude longer than the fast scale. This slow scale is generally seen to increase with the size of the lattice. In the periodic chain we see evidence for two attracting equilibria, corresponding to spatial configurations that are discrete analogues of curves that belong to the two homotopy classes of the projective plane. In open chains we typically see convergence to an equilibrium where the *Q*-tensor at the interior sites interpolates between the *Q*-tensors at the two boundary points. Additional stable equilibria are also possible, and we show an example of boundary conditions leading to two attracting equilibria of opposite helicity. The discrete Landau—de Gennes system and more general parabolic systems with a similar structure can exhibit other dynamical behaviours such as propagating fronts, see e.g. [7], these can be examined in future work.

The paper is organized as follows. In section 2, we define the discrete Landau–de Gennes and Oseen–Frank functionals and state the main results on continuation of equilibria and normally hyperbolic invariant manifolds of the decoupled system. In section 3, we review the geometry of critical sets of the decoupled Landau–de Gennes system and prove the results of the paper. In section 4, we present the numerical results on the Landau–de Gennes gradient flow in the interval and the circle. Possible extensions are discussed in section 5.

2. Discrete Landau-de Gennes system and anticontinuous limit

To define discrete Landau–de Gennes systems we first recall the continuous version. The Landau–de Gennes theory for nematic liquid crystals describes the orientational state of the liquid crystal by the "Q-tensor", a $q \times q$ symmetric traceless real matrix-valued function defined on the domain $D \subset \mathbb{R}^d$ of the liquid crystal. Typically q = d. In this work, we are interested in the case q = 3. In the numerical examples below we consider q = 3 in discretized d = 1 domains.

Static configurations in D are obtained by extremizing the Landau-de Gennes energy functional

$$\mathcal{F}_{LG}(Q) = \int_{D} \left(\frac{L}{2} |\nabla Q|^2 + f_B(Q) \right), \tag{2.1}$$

where $|\nabla Q|^2 = \sum_{i,j=1}^q \sum_{k=1}^d (\partial_{x_k} Q_{i,j})^2$, and

$$f_B(Q) = -\frac{a^2}{2} \operatorname{tr}(Q^2) - \frac{b^2}{3} \operatorname{tr}(Q^3) + \frac{c^2}{4} (\operatorname{tr}(Q^2))^2.$$
 (2.2)

L, a^2 , b^2 , c^2 are positive constants that describe the material and its state. The Dirichlet problem is obtained by varying over configurations with fixed boundary values of Q at ∂D .

A simpler model for nematic liquid crystals is the Oseen–Frank theory, where the orientation of the liquid crystal is described by the "director field", a unit vector field $\mathbf{n} \in \mathbb{R}^q$ on the domain $D \subset \mathbb{R}^d$. Static configurations are obtained by extremizing the Oseen–Frank energy functional

$$\mathcal{F}_{OF}(Q) = \frac{1}{2} \int_{D} |\nabla \mathbf{n}|^{2}, \tag{2.3}$$

where $|\nabla \mathbf{n}|^2 = \sum_{k=1}^d \sum_{i=1}^q (\partial_{x_k} \mathbf{n}_i)^2$. The Dirichlet problem is obtained by varying over configurations with fixed boundary values of \mathbf{n} at ∂D .

In this study, we are also interested in discrete versions of the theory in domains D without boundary, e.g. tori, spheres, etc., with possible modification of the quadratic part of the energy for nonflat geometries. Suitable gradient flows of $-\mathcal{F}_{LG}$, $-\mathcal{F}_{OF}$ describe the dynamics of approach to equilibria.

Discrete versions of the above systems are used in numerical computation with finite difference methods [8, 24, 32]. Energy functionals (2.1), (2.3) are widely studied special cases of more general (and realistic) Landau–de Gennes and Oseen–Frank functionals that include three elastic parameters, see e.g. [1, 14, 20, 28, 32].

The Oseen–Frank energy (2.3) can be formally obtained from the Landau–de Gennes energy (2.1) by using the "uniaxial approximation" Ansatz, see e.g. [22, 32]. The results of the paper extend [25, 26] and give a mathematical interpretation of this approximation in the limit of vanishing coupling L for both the static and dynamic problems of finite discretized versions.

In the discrete version of the Landau–de Gennes theory Q is a function on a discrete set \overline{G} that has the structure of a finite graph, i.e. a pair (\overline{G}, c) defined by a nonempty finite discrete set \overline{G} and a function $c: \overline{G} \times \overline{G} \to \{0,1\}$ satisfying c(n,n) = 0, $\forall n \in \overline{G}$, and c(n,m) = c(m,n), $\forall n, m \in \overline{G}$. The function c is the *connectivity matrix* of the graph, i.e. c(n,m) = 1 represents sites n, m that are connected by an edge.

We further consider a set $\partial G \subset \overline{G}$, and let $G = \overline{G} \setminus \partial G$. We assume that G is connected. We will consider two versions of the discrete theory: (i) ∂G is empty and the discretized functional is defined on functions on \overline{G} , and (ii) ∂G is nonempty and the discretized functional is defined on functions on G. In the second case, the values at ∂G are fixed and play the role of the boundary values.

In applications to numerical solution of the Landau–de Gennes system in domains $D \subset \mathbb{R}^d$, G and ∂G are discrete analogues of D and ∂D respectively. The use of graphs allows for more variety, e.g. lattices that discretize manifolds and branched manifolds. The notion of a boundary in the discrete problem is also more general, the boundary can be any subset of \overline{G} where we fix Q.

Let Sym_0^q denote the set of symmetric traceless $q \times q$ real matrices. The set Sym_0^q is a real linear space of dimension $d_q = q(q-1)/2 - 1$. Also, given $A \subset \overline{G}$ we let X(A) denote the set of functions $f: A \to \operatorname{Sym}_0^q$. Given A_1, A_2 disjoint subsets of \overline{G} such that $A_1 \cup A_2 = \overline{G}$ we have $X(\overline{G}) = X(A_1) \times X(A_2)$, and we may write $\overline{Q} \in X(\overline{G})$ as $\overline{Q} = [Q_1, Q_2]$ with $Q_j \in X(A_j)$.

The first discrete version of \mathcal{F}_{LG} we consider has the form

$$\overline{\mathcal{F}} = L\overline{\mathcal{F}}_2 + \overline{\mathcal{F}}_4,\tag{2.4}$$

with $\overline{\mathcal{F}}_2$, $\overline{\mathcal{F}}_4: X(\overline{G}) \to \mathbb{R}$ defined by

$$\overline{\mathcal{F}}_2(\overline{Q}) = \frac{1}{4} \sum_{n,m \in \overline{G}} c(n,m) |\overline{Q}(n) - \overline{Q}(m)|^2, \quad \overline{\mathcal{F}}_4(\overline{Q}) = \sum_{n \in \overline{G}} f_B(\overline{Q}(n)), \tag{2.5}$$

with $|M|^2 = \sum_{i,j=1}^q M_{i,j}^2$ and f_B as in (2.2).

The define the discrete analogue of equations with Dirichlet boundary data, we consider a nonempty $\partial G \subset \overline{G}$, and choose a function $Q_b : \partial D \to \operatorname{Sym}_0^q$. Let $G = \overline{G} \setminus \partial G$. We have $X(\overline{G}) = X(G) \times X(\partial G)$. Then the second discretized version of \mathcal{F}_{LG} will have the form

$$\mathcal{F} = L\mathcal{F}_2 + \mathcal{F}_4,\tag{2.6}$$

with \mathcal{F}_2 , $\mathcal{F}_4: X(G) \to \mathbb{R}$ defined by

$$\mathcal{F}_2(Q;Q_b) = \overline{\mathcal{F}}_2([Q,Q_b]), \quad \mathcal{F}_4(Q;Q_b) = \overline{\mathcal{F}}_4([Q,Q_b]), \tag{2.7}$$

with $\overline{\mathcal{F}}_2$, $\overline{\mathcal{F}}_4$ as in (2.5). The function Q_b represents the boundary data.

The discretization of the quadratic part of the energy of (2.1) by $\overline{\mathcal{F}}_2$ is indicative of more general discrete quadratic energies, e.g. with c symmetric and positive. The theory below extends to such generalizations.

We identify $X(\overline{A})$, A = G or \overline{G} , with $(\operatorname{Sym}_0^q)^{|A|} \subset (\operatorname{Mat}(q))^{|A|}$. The trace inner product $\langle R(k), S(k) \rangle = \sum_{k \in A} \operatorname{tr}(R(k)S^T(k))$, R(k), $S(k) \in \operatorname{Mat}(q)$, $k \in A$, induces a metric topology and a Riemannian metric on $(\operatorname{Mat}(q))^{|A|}$, and $(\operatorname{Sym}_0^q)^{|A|}$ in a standard way. The functionals of (2.4)-(2.5), (2.7) are real analytic in $X(\overline{G})$, X(G), respectively.

The gradient flow of $-\overline{\mathcal{F}}$ in the phase space $X(\overline{G})$ with the trace inner product is the system $\dot{\overline{Q}} = -\nabla \overline{\mathcal{F}}(\overline{Q})$. Equilibria are critical points of $\overline{\mathcal{F}}$ in $X(\overline{G})$. The gradient flow of \mathcal{F} is the system $\dot{\overline{Q}} = -\nabla_Q \mathcal{F}(Q; Q_b)$. Equilibria are critical points of \mathcal{F} in X(G).

We consider the problem of continuation of L=0 equilibria in the discrete setting. To state the results, we first classify the equilibria of the L=0 system. At L=0 the equations for the critical points of $\overline{\mathcal{F}}$, \mathcal{F} at different sites decouple and it suffices to study solutions of the d_q equations $Df_B(Q) = 0$, $Q \in \operatorname{Sym}_0^q$.

The critical points for cases q = 2, 3 are well known [12, 20, 21]. In the case q = 3, $d_q = 5$, the following [26] summarizes the result.

Proposition 2.1. The solutions of $Df_B = 0$ consist of the origin (Q = 0), and the sets

$$\Sigma_{+}^{3} := \{ Q \in Sym_{0}^{3} : Q = Q_{+}(\hat{v}) := -3x_{+}(\hat{v} \otimes \hat{v} - \frac{1}{3}I), \hat{v} \in S^{2} \},$$
 (2.8)

$$\Sigma_{-}^{3} := \{ Q \in Sym_{0}^{3} : Q = Q_{-}(\hat{v}) = -3x_{-}(\hat{v} \otimes \hat{v} - \frac{1}{3}I), \hat{v} \in S^{2} \},$$
 (2.9)

with x_+ , x_- positive and negative roots of $-a^2+6c^2x^2+b^2x=0$ respectively, I the 3×3 identity, $S^2\subset\mathbb{R}^3$ the unit sphere. Expressions (2.8), (2.9) define embeddings of the projective plane $\mathbb{R}P^2$ into Sym_0^3 , i.e. the sets Σ_\pm^3 are submanifolds of Sym_0^3 and are diffeomorphic to $\mathbb{R}P^2$. Furthermore, the infimum of f_B in Sym_0^3 is attained at Σ_-^3 , and $\nabla^2 f_B$ at Σ_-^3 has two null and three positive eigenvalues. The origin is a local maximum of f_B and is nondegenerate, while $\nabla^2 f_B$ at Σ_+^3 has null, negative and positive eigenvalues.

The set of critical points of $\overline{\mathcal{F}}_4$ is the set of maps $\Phi: \overline{G} \to 0 \cup \Sigma^3_- \cup \Sigma^3_+ \subset \operatorname{Sym}_0^3$ and consists of a finite collection of maximal connected subsets of $X(\overline{G})$. The maximal connected sets of nontrivial

critical points of \mathcal{F}_4 are labelled by pairs of disjoint subsets U_+, U_- of \overline{G} with nonempty union. Given any such pair, let $\mathcal{C}_0(\overline{\mathcal{F}}_4; U_+, U_-)$ denote the set of maps $\Phi: \overline{G} \to \operatorname{Sym}_0^3$ with the property that if $U_j \neq \emptyset$, $j \in \{+, -\}$, then $\Phi(n) \in \Sigma_j^3$, $\forall n \in U_j$, and $\Phi(n) = 0$, for all n in the complement of $U = U_+ \cup U_-$ in \overline{G} . Then $\mathcal{C}_0(\overline{\mathcal{F}}_4; U_+, U_-) = (\Sigma_+^3)^{|U_+|} \times (\Sigma_-^3)^{|U_-|}$ is a maximal connected set of critical points of $\overline{\mathcal{F}}_4$ that is diffeomorphic to $(\mathbb{R}P^2)^{|U|}$, see Lemma 3.10 of [26]. These considerations give a complete list of the manifolds of critical points of $\overline{\mathcal{F}}_4$.

Similarly, the set of critical points of \mathcal{F}_4 is the set of maps $\Phi: G \to 0 \cup \Sigma_-^3 \cup \Sigma_+^3 \subset \operatorname{Sym}_0^3$ and consists of a finite collection of maximal connected subsets of X(G). The maximal connected sets of nontrivial critical points of \mathcal{F}_4 are labelled by pairs of disjoint subsets U_+, U_- of G with nonempty union. Given any such pair we let $\mathcal{C}_0(\mathcal{F}, U_+, U_-)$ denote the set of maps $\Phi: G \to \operatorname{Sym}_0^3$ with the property that if $U_j \neq \emptyset, j \in \{+, -\}$, then $\Phi(n) \in \Sigma_j^3, \forall n \in U_j$, and $\Phi(n) = 0$, for all n in the complement of $U = U_+ \cup U_-$ in G. Then $\mathcal{C}_0(\mathcal{F}_4; U_+, U_-) = (\Sigma_+^3)^{|U_+|} \times (\Sigma_-^3)^{|U_-|}$ is a maximal connected set of critical points of \mathcal{F}_4 that is diffeomorphic to $(\mathbb{R}P^2)^{|U|}$. These considerations give a complete list of the manifolds of critical points of \mathcal{F}_4 , see also [26].

The main question is which of the L = 0 equilibria can be continued to solutions of the L > 0 problem. We present below necessary and sufficient conditions.

The new results of the paper concern the case without boundary.

Lemma 2.2. Let q = 3, then for |L| sufficiently small every nontrivial critical point of $\overline{\mathcal{F}}$ belongs to a maximal compact embedded manifold of critical points of $\overline{\mathcal{F}}$.

Thus critical points are not isolated. A manifold M of critical points of $\overline{\mathcal{F}}$ is *nondegenerate* if for every $Q \in M$, $\nabla^2 \overline{\mathcal{F}}(Q)$ has a nullspace of dimension $\dim(M)$. The manifolds that can occur as maximal sets of critical points of $\overline{\mathcal{F}}$ are classified in section 3.

We first state a necessary condition satisfied by a one-parameter family Q(L) of critical points of $\overline{\mathcal{F}}$.

Proposition 2.3. Let q = 3. Suppose there exists an $\epsilon_0 > 0$ such that $Q(L) \in Sym_0^q$ is a critical point of $\overline{\mathcal{F}} = L\overline{\mathcal{F}}_2 + \overline{\mathcal{F}}_4$, for every $L \in [0, \epsilon_0]$. Assume also that Q(L) is C^l in $[0, \epsilon_0]$ and that there exist disjoint subsets U_+ , U_- of \overline{G} , $U_+ \cup U_- \neq \emptyset$, such that $Q(0) \in \mathcal{C}_0(\overline{\mathcal{F}}_4, U_+, U_-)$. Then Q(0) is a critical point of $\overline{\mathcal{F}}_2$, restricted to $\mathcal{C}_0(\overline{\mathcal{F}}_4, U_+, U_-)$.

Thus the continued branches must be critical points of the quadratic functional $\overline{\mathcal{F}}_2$, restricted to $\mathcal{C}_0(\overline{\mathcal{F}}_4, U_+, U_-)$. The equation for these restricted critical points will be referred to as the *reduced* (or *bifurcation equation*) at L=0. The following is a sufficient condition for continuation of critical points of the L=0 problem.

Proposition 2.4. Let q=3. Let U_1 , U_2 disjoint subsets of \overline{G} with nonempty union. Suppose that \mathcal{M}_0 is a nondegenerate embedded manifold of critical points of $\overline{\mathcal{F}}_2$, restricted to $\mathcal{C}_0(\overline{\mathcal{F}}_4, U_1, U_2)$. Then there exists $\epsilon_0 > 0$ and a unique real analytic one-parameter family $\mathcal{M}(L)$, $|L| < \epsilon_0$, of embedded manifolds of critical points of $\overline{\mathcal{F}} = L\overline{\mathcal{F}}_2 + \overline{\mathcal{F}}_4$ that also satisfies $\mathcal{M}(0) = \mathcal{M}_0$.

Analogous necessary and sufficient conditions for the discrete problem with boundaries were shown in [26]. We include them below for completeness, also the numerical examples below consider geometries of both types.

Proposition 2.5. Let q = 3. Let $Q_b : \partial G \to Sym_0^q$. Suppose there exists an $\epsilon_0 > 0$ such that $Q(L) \in Sym_0^q$ is a critical point of $\mathcal{F} = L\mathcal{F}_2(Q; Q_b) + \mathcal{F}_4(Q; Q_b)$, for every $L \in [0, \epsilon_0]$. Assume also that Q(L) is C^I in $[0, \epsilon_0]$ and that there exist disjoint subsets U_I , U_2 of G, $U_1 \cup U_2 \neq \emptyset$, such that $Q(0) \in \mathcal{C}_0(\mathcal{F}_4, U_1, U_2)$. Then Q(0) is a critical point of \mathcal{F}_2 restricted to $\mathcal{C}_0(\mathcal{F}_4, U_1, U_2)$

Proposition 2.6. Let q=3. Let U_1 , U_2 be disjoint subsets of G with nonempty union. Also let $Q_b: \partial G \to \operatorname{Sym}_0^q$. Suppose that ψ_0 is a nondegenerate critical point of $\mathcal{F}_2(\cdot; Q_b)$, restricted to $\mathcal{C}_0(\mathcal{F}_4, U_1, U_2)$. Then there exists $\epsilon_0 > 0$ and a unique real analytic one-parameter family Q(L), $|L| < \epsilon_0$ of critical points of $\mathcal{F}(\cdot; Q_b) = L\mathcal{F}_2(\cdot; Q_b) + \mathcal{F}_4(\cdot; Q_b)$ that also satisfies $Q(0) = \psi_0$.

The difference between the results for graphs with and without boundary is due to symmetry. In graphs without boundary $\overline{\mathcal{F}}_2$, $\overline{\mathcal{F}}_4$ and $\overline{\mathcal{F}}$ are invariant under an action of SO(3) on $X(\overline{G})$ we describe in the next section. In graphs with boundary \mathcal{F}_2 , and \mathcal{F} do not have this symmetry because of terms that couple sites in the "interior" G and the "boundary" ∂G where the data is fixed. A consequence is that critical points of \mathcal{F} can be isolated, while nontrivial critical points of $\overline{\mathcal{F}}$ belong to manifolds obtained by the diagonal adjoint action of SO(3) on any critical point. This action is a generalization of rotations of the directions defining the projective plane, see section 2, Definition 3.9, and can be applied at all sites, see section 3.

The proofs of Propositions 2.3, 2.4 are similar to their analogues for the case with boundary Propositions 2.5, 2.6 in [26]. The main step is Lemma 3.11 on the reduction of the equation for equilibria to an equation on a product of product of projective planes. We summarize the proofs in the next section. The modifications due to the additional global SO(3) symmetry are minor. The main additional property is the equivariance of the reduced equation under the diagonal adjoint action of SO(3) on products of projective planes, see Lemma 3.12. The isotropy subgroups of this action are classified in Proposition 3.13, this result leads to a list of possible manifolds of critical points, see e.g. [16].

The most interesting critical points are local and global minima of $\overline{\mathcal{F}}_4$ and \mathcal{F}_4 . Minima correspond to the cases $U_- = \overline{G}$ for $\overline{\mathcal{F}}_4$, and $U_- = G$ for \mathcal{F}_4 . The corresponding bifurcation equation for these cases is the equation for critical points of discrete generalized Oseen–Frank functionals.

Proposition 2.7. Let q = 3. (i) Let $U_- = \overline{G}$, $U_+ = \emptyset$. Then critical points of the function $\overline{\mathcal{F}}_2$, restricted to $C_0(\overline{\mathcal{F}}_4, U_+, U_-)$, can be mapped bijectively to critical points of a discrete generalized Oseen–Frank functional $\overline{\mathcal{F}}_{2_r}: (\mathbb{R}P^2)^{|\overline{G}|} \to \mathbb{R}$ that is also invariant an action of SO(3). (ii) Let $U_- = G$, $U_+ = \emptyset$, and consider a Q_b with values in Σ_-^2 . Then critical points of the function \mathcal{F}_2 , restricted to $C_0(\mathcal{F}_4, U_+, U_-)$, can be mapped bijectively to critical points of a discrete generalized Oseen–Frank functional $\mathcal{F}_{2_r}: (\mathbb{R}P^2)^{|G|} \to \mathbb{R}$.

The generalized discrete Oseen–Frank functional $\overline{\mathcal{F}}_{2_r}$ of the proposition is given in section 3, see [26] for $\mathcal{F}_{2,r}$.

A corollary of the nondegeneracy of the critical points of f_B , Lemma 3.5, is the existence of normally hyperbolic invariant sets in the gradient flow of the Landau–de Gennes energy. The statement uses the terminology of [10].

Proposition 2.8. Let q=3. Let $r\geq 1$. (i) Let U_+,U_- be disjoint subsets of \overline{G} with nonempty union. Then the set $C_0(\overline{\mathcal{F}}_4,U_+,U_-)$ is r-normally hyperbolic under the flow of $-\nabla\overline{\mathcal{F}}_4$. Also, every point of $C_0(\overline{\mathcal{F}}_4,U_+,U_-)$ has $5|U^c|+2|U_+|$ unstable directions, and $3|U_-|+|U_+|$ stable directions, U^c the complement of $U_+\cup U_-$ in \overline{G} . (ii) Let $Q_b:\partial G\to \operatorname{Sym}_0^q$. Let U_+,U_- be disjoint subsets of G with nonempty union. Then the set $C_0(\mathcal{F}_4,U_+,U_-)$ is r-normally hyperbolic under the flow of $-\nabla_Q\overline{\mathcal{F}}_4(Q;Q_b)$. Also, every point of $C_0(\overline{\mathcal{F}}_4,U_+,U_-)$ has $5|U^c|+2|U_+|$ unstable directions, and $3|U_-|+|U_+|$ stable directions, U^c the complement of $U_+\cup U_-$ in G.

By the theory of normal hyperbolicity [3, 4, 10, 11, 15] all the invariant sets $C_0(\overline{\mathcal{F}}_4, U_+, U_-)$ and $C_0(\mathcal{F}_4, U_+, U_-)$ of the L=0 gradient flow of $\overline{\mathcal{F}}$, \mathcal{F} respectively persist for |L| sufficiently small and conserve their normal contraction and expansion properties.

The numerical study in section 4 is motivated primarily by Proposition 2.8. In the case $U = U_{-}$, $U^{c} = \emptyset$, the expected $L \neq 0$ invariant sets attract orbits in their vicinity. We expect that for L > 0 and

sufficiently small, trajectories of the gradient flows should approach the attracting invariant manifold that is parametrized by the uniaxial Q-tensors of $(\Sigma_{-}^{3})^{|U|}$, $U = \overline{G}$ or G. The numerical observations are consistent with this scenario. We see that the Q-tensor first becomes nearly uniaxial at all sites and then slowly converges to an equilibrium. The slow realignment of the director fields over this longer time scale is interpreted as motion on the invariant manifold.

The theory of the equilibria presented is a generalization of the theory developed for "breather solutions" of the discrete nonlinear Schrödinger equation [29–31, 33]. These solutions are periodic orbits of a Hamiltonian system. In the present problem the gradient structure of the dynamics allows us to approximate attracting equilibria by integrating the evolution equations. We see in section 4 that convergence is generally slow. Other tools to compute these equilibria may be used in future work, the literature on the numerical continuation and bifurcations of such solutions in is extensive.

3. Reduced equation and continuation of solutions

In this section, we prove the theoretical results of the paper and introduce notation used in the numerical study of section 4. In subsection 3.1 we review the geometry of the critical sets of f_B and the geometrical constructions used in the proofs of the main results and in section 4. The proofs are presented in subsection 3.2.

In subsection 3.1, we use the symmetry of the onsite energy f_B under rotations to analyse the geometry of its critical sets and their neighbourhood, see Definition 1 for a precise description of this symmetry. A main idea is that, due to the symmetry of the nontrivial critical sets Σ_{\pm}^3 of f_B , computations involving derivatives of f_B can be performed at any point of Σ_{\pm}^3 , see Lemmas 3.2, 3.3. This point is chosen to simplify the computations. This idea is implemented more effectively by a suitable choice of coordinates for the linear space Sym_0^3 , see Lemma 3.4. The nondegeneracy of the sets Σ_{\pm}^3 is summarized in Lemma 3.5. The remaining part of subsection 3.1 uses the symmetry to define a special system of coordinates for tubular neighbourhoods of the nontrivial critical sets Σ_{\pm}^3 of f_B , see Remarks 3.7, 3.8 and Lemma 3.9 for their properties.

In subsection 3.2, we use this construction to define analogous systems of coordinates for tubular neighbourhoods of the anticontinuous limit critical sets of \mathcal{F} . We use the fact that these sets are products of the Σ^3_{\pm} . The use of these coordinates greatly simplifies the computations needed to show key Lemma 3.11 on the reduced equations, and its consequences, Propositions 2.3, 2.4. The same computation is also the main step to show Propositions 2.7, 2.8. In the case without boundary the reduced energy has an additional global symmetry, see Lemma 3.12. This implies the possibility of manifolds of critical points of the reduced equations, Proposition 3.13 leads to their classification.

3.1. Critical sets of the onsite energy f_B and their geometry

We review the polar coordinate system for 3×3 *Q*-tensors and the classification of the critical points of f_B , summarized in Lemma 3.1. We also review an alternative system of coordinates that is used to describe the neighbourhood of the critical sets of f_B . The construction uses the invariance of f_B under the adjoint action of the rotation group, see Definition 1.

For any $Q \in \operatorname{Sym}_0^3$ we have the spectral decomposition

$$Q = \lambda_1 \hat{n} \otimes \hat{n} + \lambda_2 \hat{m} \otimes \hat{m} + \lambda_3 \hat{p} \otimes \hat{p}, \tag{3.1}$$

with $\lambda_1 \geq \lambda_2 \geq \lambda_3$ the eigenvalues of Q, and \hat{n} , \hat{m} , $\hat{p} \in \mathbb{R}^3$ the corresponding orthonormal system of eigenvectors. In the case $\lambda_1 > \lambda_2 > \lambda_1$ the vectors \hat{n} , \hat{m} , \hat{p} are determined uniquely up to signs.

Since Q is traceless, we have $\lambda_3 = -\lambda_1 - \lambda_2$ and we see that

$$Q = s(\hat{n} \otimes \hat{n} - \frac{1}{3}I) + r(\hat{m} \otimes \hat{m} - \frac{1}{3}I), \tag{3.2}$$

8

where

$$s = 2\lambda_1 + \lambda_2, \quad r = 2\lambda_2 + \lambda_1, \tag{3.3}$$

and I is the 3×3 identity matrix.

We examine the range of values the λ_1 , λ_2 , assuming $\lambda_1 \ge \lambda_2 \ge \lambda_3$. The case $\lambda_1 = 0$ implies $\lambda_2 = \lambda_3 = 0$, and corresponds to Q = 0.

If $\lambda_1 \neq 0$ the trace condition implies $\lambda_1 > 0$ and $\lambda_3 < 0$. Considering any $\lambda_1 > 0$, the values of λ_2 belong to two intervals: region *I* where $\lambda_1 \geq \lambda_2 \geq 0 > \lambda_3$, and region *II* where $\lambda_1 > 0 > \lambda_2 \geq \lambda_3$.

In region *I*, we have $\lambda_2 \in [0, \lambda_1]$, and by (3.3), $r \in [s/2, s]$, with $s \in [2\lambda_1, 3\lambda_1]$.

In region *II*, we have $\lambda_2 \in [-\lambda_1/2, 0)$, and by (3.3), $r \in [0, s/2)$, $s \in [3/2\lambda_1, 2\lambda_1)$.

The boundaries of regions *I*, and *II* intersect at $\lambda_2 = 0$. The second (upper) boundary of interval *I*, $\lambda_2 = \lambda_1$, corresponds to $r = s = 3\lambda_1$. In that case, by (3.2) we have

$$Q = -s(\hat{p} \otimes \hat{p} - \frac{1}{3}I) = -3\lambda_1(\hat{p} \otimes \hat{p} - \frac{1}{3}I). \tag{3.4}$$

The second (lower) boundary of interval II, $\lambda_2 = -\frac{1}{2}\lambda_1 = \lambda_3$, corresponds to r = 0, $s = \frac{3}{2}\lambda_1 = -3\lambda_2$. Then

$$Q = s(\hat{n} \otimes \hat{n} - \frac{1}{3}I) = -3\lambda_2(\hat{n} \otimes \hat{n} - \frac{1}{3}I). \tag{3.5}$$

Recall that Q is termed *uniaxial* if it has two equal nonzero eigenvalues, and *isotropic* if Q = 0. Otherwise Q is *biaxial*. The uniaxial Q-tensors correspond to the boundary of the union of regions I and II.

Lemma 3.1. Let x_+ , x_- denote the positive and negative roots of

$$-a^2 + 6c^2x^2 + b^2x = 0, (3.6)$$

respectively. Then the critical points of f_B consist of the sets defined by

- (i) $\lambda_1 = \lambda_2 = 0$, where Q = 0,
- (ii) $\lambda_1 > 0$ with $r = s = 3\lambda_1 > 0$ (upper boundary of region I), where

$$Q = -3x_{+}(\hat{p} \otimes \hat{p} - \frac{1}{3}I), \quad \hat{p} \in S^{2} \subset \mathbb{R}^{3}, \tag{3.7}$$

(iii) $\lambda_1 > 0$ with r = 0, $s = \frac{3}{2}\lambda_1$ (lower boundary of region II), where

$$Q = -3x_{-}(\hat{n} \otimes \hat{n} - \frac{1}{3}I), \quad \hat{n} \in S^{2} \subset \mathbb{R}^{3}.$$

$$(3.8)$$

The infimum of f_B is attained at the set (iii), denoted by Σ_-^3 . The set (ii) is denoted by Σ_+^3 and is not a set of local extrema of f_B . The results are summarized by Proposition 2.1, see [20, 21, 26] for details.

In the polar representation the value of r quantifies the deviation from the set of uniaxial tensors Σ_{\pm}^3 . However, the polar representation is singular at the critical points of f_B , and we need alternative systems of coordinates for the neighbourhood of the sets Σ_{\pm}^3 . The system of coordinates we define below is motivated by the symmetries of f_B . We recall the following.

Definition 1. Given $A \in SO(3)$, we define Ψ_A on the set Mat(3) of real 3×3 matrices by

$$\Psi_A(Q) = AQA^T = AQA^{-1}. (3.9)$$

Also define $\Psi : SO(3) \times Mat(3) \rightarrow Mat(3)$ by $\Psi(A, Q) = \Psi_A(Q)$.

Lemma 3.2. Let $A \in SO(3)$, then $\Psi_A : Mat(3) \to Mat(3)$ is an invertible linear transformation that preserves Sym_0^3 . Furthermore $f_B : Sym_0^3 \to \mathbb{R}$ is invariant under Ψ_A .

The restrictions of the Ψ_A , $A \in SO(3)$, to Sym_0^3 , and Ψ to $SO(3) \times \operatorname{Sym}_0^3$ are denoted by Ψ_A , Ψ , respectively.

By Lemma 3.2 the maps Ψ_A , $A \in SO(3)$, in Mat(3), Sym_0^3 can be represented by matrix multiplication in \mathbb{R}^9 , \mathbb{R}^5 , respectively. The matrices depend on the choice of basis in Mat(3), Sym_0^3 , respectively.

Consider a basis $\{\hat{W}_j\}_{j=1}^5$ in Sym_0^3 , with $Q = \sum_{j=1}^5 w_j \hat{W}_j$, $\forall Q \in \operatorname{Sym}_0^3$, and the isomorphism $\overline{\beta}^w(Q) = w := [w_1, \dots, w_5]^T \in \mathbb{R}^5$. Then the matrix representation of Ψ_A , $A \in SO(3)$, in this basis is the unique matrix T_A^w satisfying $T_A^w(\overline{\beta}^w(Q)) = \overline{\beta}^w(\Psi_A(Q))$. T_A^w has inverse $T_{A^{-1}}^w$, $\forall A \in SO(3)$. Also define $T^w : SO(3) \times \mathbb{R}^5 \to \mathbb{R}^5$ by $T^w(A, q) = T_A^w q$.

The application of the actions Ψ , T^w to the analysis of the critical sets of f_B is based on the following observations, see [26] for more details.

Lemma 3.3. The sets Σ^3_{\pm} are invariant under Ψ , moreover the orbit of any point of Σ^3_{\pm} under Ψ is Σ^3_{\pm} . Also, let $\overline{\beta}^w$: $Sym_0^3 \to \mathbb{R}^5$ be an isomorphism, then the sets $\overline{\beta}^w(\Sigma^3_{\pm})$ are invariant under T^w , moreover the orbit of any point of $\overline{\beta}^w(\Sigma^3_{\pm})$ under T^w is $\overline{\beta}^w(\Sigma^3_{\pm})$.

The lemma is used to simplify computations in the neighbourhood of the sets $\overline{\beta}^w(\Sigma_{\pm}^3)$. In particular, we can compute quantities of interest related to the derivative of f_B at a single point and use the properties of T^w to extend the result to all points of $\overline{\beta}^w(\Sigma_{\pm}^3)$.

To implement this idea it is also convenient to define bases of Mat(3) that lead to a representation of the Ψ_A , $A \in SO(3)$, and Ψ , restricted to Sym_0^3 , by rotation matrices. This construction allows us to understand the local geometry of the critical sets of f_B by computations at a single point. This point is chosen below to further simplify the computations.

Consider first the standard basis of Mat(3) of matrices $\hat{Q}_{i,j}$ with i,jth entry unity and all other entries zero. We let $\hat{Z}_k = \hat{Q}_{i,j}$, where the enumeration k(i,j) is defined by

$$Q = \begin{bmatrix} z_1 & z_2 & z_3 \\ z_4 & z_5 & z_6 \\ z_7 & z_8 & z_9 \end{bmatrix}, \quad Q = \sum_{k=1}^9 z_k \hat{Z}_k.$$
 (3.10)

We define the inner product $\langle \cdot, \cdot \rangle$ in Mat(3) by $\langle R, S \rangle = \operatorname{tr}(RS^T) = \sum_{k=1}^9 r_k s_k$, $R = \sum_{k=1}^9 r_k \hat{Z}_k$, $S = \sum_{k=1}^9 s_k \hat{Z}_k$. The corresponding norm is denoted by $||\cdot||$.

The isomorphism $\beta^z: \operatorname{Mat}(3) \to \mathbb{R}^9$ defined by $\beta^z(Q) = z := [z_1, \ldots, z_9]^T$, $Q = \sum_{k=1}^9 z_k \hat{Z}_k$, is an isometry between $\operatorname{Mat}(3)$ with $||\cdot||$, and \mathbb{R}^9 with the Euclidean norm. The map Ψ_A , $A \in SO(3)$, is represented by multiplication by the matrix $[\Psi_A]^z$, that is $\beta^z(\Psi_A(Q)) = [\Psi_A]^z\beta^z(Q)$, $\forall Q \in \operatorname{Mat}(3)$. Then $[\Psi_A]^z$ is orthogonal in \mathbb{R}^9 with the Euclidean norm, $\forall A \in SO(3)$, see [26]. Consider a new basis $\{\hat{Y}_j\}_{j=1}^9$ of $\operatorname{Mat}(3)$, let $Q = \sum_{k=1}^9 y_k \hat{Y}_k$, $\forall Q \in \operatorname{Mat}(3)$, and define the isomor-

Consider a new basis $\{Y_j\}_{j=1}^g$ of Mat(3), let $Q = \sum_{k=1}^g y_k Y_k$, $\forall Q \in \text{Mat}(3)$, and define the isomorphism $\beta^y : \text{Mat}(3) \to \mathbb{R}^9$ by $\beta^y(Q) = y := [y_1, \dots, y_9]^T$. Assume that (i): $\hat{Y}_i = \sum_{j=1}^g M_{i,j} \hat{Z}_j$, with M an orthogonal matrix with respect to the Euclidean inner product on \mathbb{R}^9 , and (ii): $Q \in \text{Sym}_0^3$ if and only if $(\beta^y(Q))_i = 0$, for $i \in \mathcal{I}, \mathcal{I} \subset \{1, \dots, 9\}$, $|\mathcal{I}| = 4$.

Denote the matrix representation of Ψ_A in the basis $\{\hat{Y}_j\}_{j=1}^9$ by $[\Psi_A]^y$. Let the matrix T_A that represents the restriction of Ψ_A to Sym_0^3 in the basis $\{\hat{Y}_j\}_{j\in\mathcal{J}}$, $\mathcal{J}=\{1,\ldots,9\}\setminus\mathcal{I}$. We can show the following, see [26].

Lemma 3.4. Multiplication by T_A , $A \in SO(3)$, is an isometry in \mathbb{R}^5 with the Euclidean norm.

An example of a basis $\{\hat{Y}_j\}_{j=1}^9$ satisfying (i), (ii) is defined by

$$y_2 = \frac{1}{\sqrt{2}}(z_2 + z_4), \quad y_4 = \frac{1}{\sqrt{2}}(z_2 - z_4),$$
 (3.11)

$$y_3 = \frac{1}{\sqrt{2}}(z_3 + z_7), \quad y_7 = \frac{1}{\sqrt{2}}(z_3 - z_7),$$
 (3.12)

$$y_6 = \frac{1}{\sqrt{2}}(z_6 + z_8), \quad y_8 = \frac{1}{\sqrt{2}}(z_6 - z_8),$$
 (3.13)

$$y_9 = \frac{1}{\sqrt{3}}(z_1 + z_5 + z_9), \quad y_1 = \frac{1}{\sqrt{2}}(z_1 - z_5), \quad y_5 = \frac{1}{\sqrt{6}}(z_1 + z_5 - 2z_9).$$
 (3.14)

Thus $Q \in \operatorname{Sym}_0^3$ is equivalent to

$$y_4 = y_7 = y_8 = y_9 = 0$$
,

i.e. $\mathcal{J} = \{1, 2, 3, 5, 6\}.$

The onsite energy f_B of (2.2) in terms of y_j , $j \in \mathcal{J}$, is then computed from

$$tr(Q^2) = y_1^2 + y_2^2 + y_3^2 + y_5^2 + y_6^2,$$
(3.15)

$$\operatorname{tr}(Q^3) = \frac{3}{\sqrt{6}}y_2^2y_5 + \frac{3}{\sqrt{2}}y_2y_3y_6 + \frac{3}{2\sqrt{2}}(y_3^2y_1 - y_6^2y_1) - \frac{3}{2\sqrt{6}}(y_3^2y_5 + y_6^2y_5) - \frac{1}{\sqrt{6}}y_5^3 + \frac{3}{\sqrt{6}}y_1^2y_5. \tag{3.16}$$

The critical sets Σ^{\pm} of f_B can be also parametrized by polar coordinates. Using

$$\hat{n}(\theta,\phi) = [\sin\theta\cos\phi, \sin\theta\sin\phi, \cos\theta]^T, \quad (\theta,\phi) \in (0,\pi) \times [0,2\pi), \tag{3.17}$$

for unit vectors in \mathbb{R}^3 , $\hat{n} \in S^2 \setminus \{\hat{e}_1, -\hat{e}_1\}$, the corresponding Q-tensors are

$$Q_{\pm}(\hat{n}(\theta,\phi)) = -3x_{\pm} \begin{bmatrix} \sin^{2}\theta\cos^{2}\phi - \frac{1}{3} & \frac{1}{2}\sin^{2}\theta\sin2\phi & \frac{1}{2}\sin2\theta\cos\phi \\ \frac{1}{2}\sin^{2}\theta\sin2\phi & \sin^{2}\theta\sin^{2}\phi - \frac{1}{3} & \frac{1}{2}\sin2\theta\sin\phi \\ \frac{1}{2}\sin2\theta\cos\phi & \frac{1}{2}\sin2\theta\sin\phi & \cos^{2}\theta - \frac{1}{3} \end{bmatrix}, \quad (3.18)$$

see (2.8), (2.9). By (3.10) and (3.11)-(3.14) their coordinates in the variables $y_i, j \in \mathcal{J}$, are

$$y_1^{\pm} = -\frac{3x_{\pm}}{\sqrt{2}}\sin^2\theta(\cos^2\phi - \sin^2\phi), \quad y_2^{\pm} = -\frac{3x_{\pm}}{\sqrt{2}}\sin^2\theta\sin2\phi, \quad y_3^{\pm} = -\frac{3x_{\pm}}{\sqrt{2}}\sin2\theta\cos\phi,$$

$$y_5^{\pm} = -\frac{3x_{\pm}}{\sqrt{6}}(\sin^2\theta - 2\cos^2\theta), \quad y_6^{\pm} = -\frac{3x_{\pm}}{\sqrt{2}}\sin 2\theta \sin \phi.$$
 (3.19)

These expressions can be used to produce local coordinates for $\mathbb{R}P^2$ and to describe its embedding to Sym_0^3 , details are given below.

In the remaining part of this subsection, we construct coordinates for a tubular neighbourhood of the critical sets Σ_{\pm}^3 of f_B . The results and notation are used in the proofs of subsection 3.2. The construction uses the spectral decomposition of $\nabla^2 f_B$.

Let $Q \in \operatorname{Sym}_0^3$, then $Q = \sum_{k=1}^5 w_j \hat{W}_j$, with

$$\hat{W}_1 = \hat{Y}_1, \quad \hat{W}_2 = \hat{Y}_2, \quad \hat{W}_3 = \hat{Y}_3, \quad \hat{W}_4 = \hat{Y}_5, \quad \hat{W}_5 = \hat{Y}_6.$$
 (3.20)

Define $\overline{\beta}^w$: Sym₀³ $\to \mathbb{R}^5$ by $\overline{\beta}^w(Q) = w := [w_1, \dots, w_5]^T$. The maps Ψ_A are represented by multiplication by the matrix T_A^w , and $(T_A^w)_{i,j} = \langle [\Psi_A]^y \hat{W}_j, \hat{W}_i \rangle$, $i, j = 1, \dots, 5$, i.e. T_A^w coincides with T_A , assuming the enumeration of \mathcal{J} in (3.20). The trace inner product $\langle \cdot, \cdot \rangle$ in Sym₀³ is given by $\langle w, w' \rangle = \sum_{i=1}^5 w_i w_i' = \sum_{j \in \mathcal{J}}^5 y_j y_j'$. Lemma 3.4 implies that multiplication by T_A^w is an isometry, $\forall A \in SO(3)$.

The application of the rotations Ψ_A , and their representation by orthogonal matrices to the analysis of the critical points of f_B is a consequence of the following observations.

Let $\mathcal{L} = f_B \circ \overline{\gamma}^w : \mathbb{R}^5 \to \mathbb{R}$, $\overline{\gamma}^w = (\overline{\beta}^w)^{-1}$, and $h : \mathbb{R}^5 \to \mathbb{R}^5$ defined by $h(q) = T_A^w q$, $A \in SO(3)$. We have that q a critical point of \mathcal{L} implies that h(q) is also a critical point of \mathcal{L} , moreover the Hessians of at q, h(q) are related by

$$(\nabla^2 \mathcal{L})(q) = [Dh(q)]^T [(\nabla^2 \mathcal{L})(h(q))][Dh(q)]. \tag{3.21}$$

Thus to check that Σ^3_{\pm} are critical sets, it suffices to check that Df_B vanishes at any point of Σ^3_{\pm} . Also, since the Hessians of \mathcal{L} at Q, $Q' = \Psi_A(Q) \in \Sigma^3_{\pm}$, $A \in SO(3)$, are related by (3.21) the spectrum of the Hessian is then same at all points of the two nontrivial critical sets of \mathcal{L} . Also, the fact that T_A^w is an isometry implies that if v an eigenvector of $(\nabla^2 \mathcal{L})(q)$ then Dh(q)v an eigenvector of $(\nabla^2 \mathcal{L})(h(q))$, corresponding to the same eigenvalue. The computation of the spectral data of $\nabla^2 \mathcal{L}$ is summarized by the following.

Lemma 3.5. The origin is a nondegenerate critical point of f_B in Sym_0^3 and is a local maximum. The two sets of nontrivial critical points of f_B in Sym_0^3 are given by the uniaxial Q-tensors of (3.7), (3.8) and are nondegenerate. The Hessian at the points of (3.8) has two zero eigenvalues and three positive eigenvalues, while the Hessian at the points of (3.7) has two zero eigenvalues, two negative eigenvalues and one positive eigenvalue. The normal subspace is spanned by the eigenvector $[\sqrt{3},0,0,1,0]^T$ that corresponds to the eigenvalue $b^2x_{\pm} + 12c^2x_{\pm}^2$ and is colinear to the solution $y^B(Q_{\pm})$ of (3.22), and the two-dimensional eigenspace corresponding to the double eigenvalue $-3b^2x_{\pm}$.

The proof follows from computations of the *Q*-tensors (3.7), (3.8) obtained from $\hat{p} = \hat{n} = \hat{e}_1 := [1,0,0]^T$ respectively, see [26]. By (3.17), (3.11)-(3.14) these critical points are

$$y_1 = -\frac{3}{\sqrt{2}}x_{\pm}, \quad y_5 = -\frac{3}{\sqrt{6}}x_{\pm}, \quad y_2 = y_3 = y_6 = 0.$$
 (3.22)

The Hessian of $\mathcal{L} = f_B \circ \overline{\gamma}^w$ at this point is simplified and its eigenvalues and eigenvectors are computed explicitly.

We use the information of Lemma 3.5 to describe the sets Σ^3_{\pm} as the image of embeddings of the projective plane to Sym_0^3 , and to construct a normal sets of coordinates in the neighbourhood of the Σ^3_{\pm} . The projective plane $\mathbb{R}P^2$ is the set of points of the 2-sphere S^2 with antipodal points identified,

The projective plane $\mathbb{R}P^2$ is the set of points of the 2-sphere S^2 with antipodal points identified, i.e. pairs $\{n, -n\}$, $n \in S^2$, with $\{n, -n\} = \{n', -n'\}$, $n, n' \in S^2$, if and only if n = n' or -n'. Equivalently, $\mathbb{R}P^2$ is the set of projectors $\hat{v} \otimes \hat{v}$, $\hat{v} \in S^2$, see e.g. [17], p.18, for the topology in each description.

Consider the maps $Q_{\pm}: S^2 \to \operatorname{Sym}_0^3 \subset \operatorname{Mat}(3)$ defined in (2.8), (2.9). We have $Q_{\pm}(-\hat{v}) = Q_{\pm}(\hat{v})$. Define $\tilde{Q}_{\pm}: \mathbb{R}P^2 \to \operatorname{Sym}_0^3$ by $\tilde{Q}_{\pm}(\{\hat{n}, -\hat{n}\}) := Q_{\pm}(\hat{n})$, and let

$$\Gamma_{+} := \overline{\beta}^{y} \circ Q_{+} : S^{2} \to \mathbb{R}^{5}, \quad \tilde{\Gamma}_{+} := \overline{\beta}^{y} \circ \tilde{Q}_{+} : \mathbb{R}P^{2} \to \mathbb{R}^{5}.$$
 (3.23)

Then $\Sigma^3_{\pm} = \tilde{Q}_{\pm}(\mathbb{R}\mathrm{P}^2)$.

To study these maps locally we define a chart in a neighbourhood \mathcal{U} of $\hat{e}_1 \in S^2$ and its antipodal points, and compose with rotations to cover $\mathbb{R}P^2$. We further use this idea to construct tangential and normal coordinates for points in the neighbourhood of the critical sets $\Sigma^3_{\pm} \subset \operatorname{Sym}^3_0$: we first construct normal coordinates for points in \mathcal{U} and then apply the matrices representing rotations to translate the normal basis vectors to all other critical points. Furthermore, our choice of tangential and normal coordinates for the neighbourhood of \mathcal{U} makes the Hessian of f_B diagonal at all points of the critical sets. This simplifies the computations of the next section.

Let \mathcal{U} be the set of unit vectors

$$\hat{n}(\theta, \phi) = [\sin \theta \cos \phi, \sin \theta \sin \phi, \cos \theta]^T \in \mathbb{R}^3, \quad (\theta, \phi) \in B,$$
(3.24)

where

$$(\theta, \phi) \in B = (\pi/2 - \Delta, \pi/2 + \Delta) \times (-\Delta, \Delta). \tag{3.25}$$

Choose Δ small enough so that \mathcal{U} does not contain antipodal points. The set \mathcal{U} is an open neighbourhood of $\hat{e}_1 = [1, 0, 0]^T \in S^2$. The inverse $\psi_1 := \hat{n}^{-1}$ of $\hat{n} : B \to \mathcal{U}$ is a coordinate chart for $\mathcal{U} \in S^2$. Given a pair of antipodal points $\{m, -m\}$, with m or $-m \in \mathcal{U}$, we identify the unique point that belongs to \mathcal{U} and map it to B via ψ_1 . This defines a function (chart) from $\tilde{\mathcal{U}} = \{\mathcal{U}, -\mathcal{U}\}$ that we denote by $\tilde{\psi}_1$.

We generate charts around other points of S^2 and $\mathbb{R}P^2$ using rotations of $\mathcal{U}, \tilde{\mathcal{U}}$.

Letting $\hat{v} \in S^2$, we let $H^{\pm}(v)$ denote the open hemisphere of unit vectors $\hat{\mu}$ satisfying $\hat{\mu} \cdot \hat{v} \geq 0$. Consider a collection $\{A_p\}_{p \in \mathcal{K}}$ of matrices $A_p \in SO(3)$, $\forall p \in \mathcal{K}$, where $\mathcal{K} \subset \mathbb{N}$ is an index set with the properties $1 \in \mathcal{K}$, $A_1 = I$, the identity matrix, and that the sets $\{A_p\mathcal{U}, -A_p\mathcal{U}\}$, $p \in \mathcal{K}$, form a cover of of $\mathbb{R}P^2$. The set \mathcal{K} can be assumed finite by compactness. We use the notation $\mathcal{U}_p = A_p\mathcal{U}$.

Given $p \in \mathcal{K}$, and the rotation matrix A_p , define $\hat{n}_p : B \to \mathcal{U}_p$ by $\hat{n}_p = A_p \hat{n}$, and let $\psi_p = \hat{n}_p^{-1} : \mathcal{U}_p \to B$. ψ_p is a coordinate chart on $\mathcal{U}_p \subset S^2$. The \hat{n}_p are real analytic and injective in B, therefore the ψ_p are also real analytic in \mathcal{U}_p , $\forall p \in \mathcal{K}$. Given the set $\tilde{\mathcal{U}}_p = \{\mathcal{U}_p, -\mathcal{U}_p\}$ define the chart $\tilde{\psi}_p : \tilde{\mathcal{U}}_p \to B$ by letting $\tilde{\psi}_p(\{m, -m\}) = \psi_p(m)$ if $m \in H^+(A_p\hat{e}_1)$, and $\tilde{\psi}_p(\{m, -m\}) = \psi_p(-m)$ if $-m \in H^+(A_p\hat{e}_1)$. Given $m \in \tilde{\mathcal{U}}_p$, $p \in \mathcal{K}$, we use the notation $(\theta_p, \phi_p) = (\theta_p(m), \phi_p(m)) = (\tilde{\psi}_{p,1}(m), \tilde{\psi}_{p,2}(m)) = (\tilde{\psi}_{p,1}, \tilde{\psi}_{p,2})$ for the two components of the chart $\tilde{\psi}_p$, i.e. we use the same symbol for the charts and the variables. For p = 1 we have $(\theta_1, \phi_1) = (\theta, \phi)$.

To see the transition functions consider $\tilde{\mathcal{U}}_p$, $\tilde{\mathcal{U}}'_p \subset \mathbb{R}\mathrm{P}^2$, $p, p' \in \mathcal{K}$ with nonempty intersection. Then either $\mathcal{U}_p \cap \mathcal{U}_{p'} \neq \emptyset$ or $\mathcal{U}_p \cap (-\mathcal{U}_{p'}) \neq \emptyset$ (and not both). Let $\mathcal{V}_{p'}$ be the element of the pair $\mathcal{U}_{p'}$, $-\mathcal{U}_{p'}$ that intersects \mathcal{U}_p . Then $\mathcal{V}_p = A'_{p'}\mathcal{U}$, for some $A'_{p'} \in SO(3)$, and

$$\hat{n}(\theta_{p'}, \phi_{p'}) = (A'_{p'})^{-1} A_p \hat{n}(\theta_p, \phi_p). \tag{3.26}$$

The transition function $\tilde{\psi}_{p'} \circ \tilde{\psi}_p^{-1} : \tilde{\psi}_p(\tilde{\mathcal{U}}_p \cap \tilde{\mathcal{U}}_{p'}) \to \tilde{\psi}_{p'}(\tilde{\mathcal{U}}_p \cap \tilde{\mathcal{U}}_{p'})$ is the map from $(\theta_p, \phi_p) \in \tilde{\psi}_p(\tilde{\mathcal{U}}_p \cap \tilde{\mathcal{U}}_{p'}) \subset B$ to the unique $(\theta_{p'}, \phi_{p'}) \in \tilde{\psi}_{p'}(\tilde{\mathcal{U}}_p \cap \tilde{\mathcal{U}}_{p'}) \subset B$ satisfying (3.26). Real analyticity of the transition function follows from the fact that the right hand side of (3.26), and \hat{n}^{-1} are real analytic.

Remark 3.6. By (3.24) we have $\hat{n}(\theta, \phi) = A_{\phi}A_{\theta}\hat{e}_1$, and \mathcal{U} is the set of $A\hat{e}_1$, $A = A_{\phi}A_{\theta}$, where $(\theta, \phi) \in B$,

$$A_{\phi} = \begin{bmatrix} \cos \phi & -\sin \phi & 0 \\ \sin \phi & \cos \phi & 0 \\ 0 & 0 & 1 \end{bmatrix}, \quad A_{\theta} = \begin{bmatrix} \sin \theta & 0 & -\cos \theta \\ 0 & 1 & 0 \\ \cos \theta & 0 & \sin \theta \end{bmatrix}.$$
 (3.27)

Part of the statement of Proposition 2.1 is that the $\tilde{\Gamma}_{\pm}$ are embeddings, see [26]. We can then define tubular neighbourhoods of their image $\overline{\beta}^{y}(\Sigma_{\pm}^{3})$ using the atlas $\{\tilde{\mathcal{U}}_{p}, \tilde{\psi}_{p}\}_{p \in \mathcal{K}}$ for the component along the $\overline{\beta}^{y}(\Sigma_{\pm}^{3})$, and coordinates along normal directions, see [17], ch. 3, [6], section 6.2.

In particular, given any $p \in \mathcal{K}$, and the open set $\tilde{\mathcal{U}}_p \in \mathbb{R}P^2$, there exists an open neighbourhood of $\tilde{\Gamma}_{\pm}(\tilde{\mathcal{U}}_p)$ in \mathbb{R}^5 that consists of points

$$y^{\pm}(\tilde{\psi}_{p}, r_{p}) = \tilde{\Gamma}_{\pm}(\theta_{p}, \phi_{p}) + \sum_{j=1}^{3} r_{p,j} \hat{N}_{p,j}^{\pm}(\theta_{p}, \phi_{p}), \quad \tilde{\psi}_{p} = (\theta_{p}, \phi_{p}) \in B, \quad r \in I_{\delta}^{3},$$
 (3.28)

 $I_{\delta} = (-\delta, \delta), \, \delta > 0, \, \tilde{\psi}_p = (\theta_p, \phi_p), \, r_p = (r_{p,1}, r_{p,2}, r_{p,3}), \, B \text{ as in (3.25), (3.24), where the } \hat{N}_{p,j}^{\pm} : \tilde{\mathcal{U}}_p \to S^5, \, j = 1, 2, 3 \text{ are smooth unit vector fields that are normal to } \tilde{\Gamma}_{\pm}(\tilde{\mathcal{U}}_p) \text{ with respect to the Euclidean inner product in } \mathbb{R}^5.$

The local normal vector fields $\hat{N}_{p,j}^{\pm}$ of (3.28) are not unique. We choose normal vectors that are eigenvectors of $\nabla^2 f_B$, see Lemma 3.9 below. This choice simplifies the proof of Lemma 3.11 in the next section, see [26] for details.

Define first local normal vector fields $N_{1,j}^{\pm}:\mathcal{U}\to S^5, j=1,2,3$: let $N_1^{\pm}(\pi/2,0)=||\Gamma_{\pm}(\hat{e}_1)||^{-1}\Gamma_{\pm}(\hat{e}_1)$, and choose two unit vectors $N_j^{\pm}(\pi/2,0), j=2,3$, so that $N_j^{\pm}(\pi/2,0), j=1,2,3$ form a orthonormal basis of the orthogonal complement of the tangent space of $\Gamma_{\pm}(\mathcal{U}_p)$ at at $\Gamma_{\pm}(\hat{e}_1)$. (The choice of the $N_j^{\pm}(\pi/2,0), j=2,3$ is not unique.) Also let

$$N_{1,j}^{\pm}(\theta,\phi) = T_{A_{\theta}A_{\phi}}N_{j}^{\pm}(\pi/2,0), \quad j=1,2,3, \quad (\theta,\phi) \in B.$$
 (3.29)

We then define the $\hat{N}_{p,j}^{\pm}: \tilde{\mathcal{U}}_p \to S^5$ by

$$\hat{N}_{p,j}^{\pm}(\{\psi_p, -\psi_p\}) = T_{A_p} N_{1,j}^{\pm}(\psi_1), \qquad \tilde{\psi}_1 \in B, \quad j = 1, 2, 3, \quad p \in \mathcal{K}.$$
(3.30)

By Lemma 3.5, and Remark 3.6 the $\hat{N}_j^{\pm}(p,m)$ are real analytic vector fields and form an orthonormal set of eigenvectors of $\nabla^2 f_B$ at $m \in \tilde{\mathcal{U}}_p$ corresponding to λ_j^{\pm} , j=1,2,3, respectively, for all $m \in \tilde{\mathcal{U}}_p$, $p \in \mathcal{K}$.

Recall that the matrices T_A , $A \in SO(3)$, represent rotations in the basis y and leave the image of $\overline{\beta}^y(\operatorname{Sym}_0^3)$ invariant. The following show that the particular choice of normal coordinates for \mathcal{U} , and its extension to the whole critical set by rotations makes the Hessian of f_B diagonal everywhere in the critical set.

Remark 3.7. Let $\Omega_p^{\pm} = (\tilde{\psi}_p, r_p^{\pm}) \in B \times I_{\delta}^3$, where B, I_{δ} are defined in (3.25)-(3.24), and (3.28) respectively. Then (3.28)-(3.29) imply

$$D_{\Omega_p} y^{\pm}(\tilde{\psi}_p, 0) = [t_{\theta_p}^{\pm}, t_{\phi_p}^{\pm}, \hat{N}_{p,1}^{\pm}, \hat{N}_{p,2}^{\pm}, \hat{N}_{p,3}^{\pm}](\tilde{\psi}_p, 0), \tag{3.31}$$

where $t_{\theta_p}^{\pm}(\tilde{\psi}_p,0), t_{\phi_p}^{\pm}(\tilde{\psi}_p,0)$ are tangent to the critical set at $(\tilde{\psi}_p,0)$, and the $\hat{N}_j^{\pm}(\tilde{\psi}_p,0)$ are normal to the critical set at $(\tilde{\psi}_p,0)$. Thus $D_{\Omega_p}y^{\pm}(\tilde{\psi}_p,0)$ is invertible and it follows that the map defined by (3.28) is an analytic diffeomorphism from $B \times I_{\delta}^3$ to an open subset of \mathbb{R}^5 that intersects $\tilde{\Gamma}(\tilde{\mathcal{U}}_p)$.

Remark 3.8. By (3.28), the linearity of T_A , and (3.30)-(3.29), the transition function between components r_p , $r_{p'}$ for any neighborhood of $\tilde{\mathcal{U}}_p \cap \tilde{\mathcal{U}}_{p'} \neq \emptyset$ is the identity, $\forall p, p' \in \mathcal{K}$. It similarly follows that the angular component of $T_A y^{\pm}(\tilde{\psi}_p, r_p)$, $r_p \in I_{\delta}^3$, depends only on $\tilde{\psi}_p$. Also, the radial component of $T_A y^{\pm}(\tilde{\psi}_p, r_p)$, $r_p \in I_{\delta}^3$, is r_p .

Lemma 3.9. Let $m \in \tilde{\mathcal{U}}_p \subset \mathbb{R}P^2$, $p \in \mathcal{K}$. Define the coordinates $\Omega_p^{\pm} = (\tilde{\psi}_p, r_p^{\pm}) \in B \times I_{\delta}^3$, by (3.28) in the neighbourhoods $y^{\pm}(B \times I_{\delta}^3)$ of $\tilde{\Gamma}_{\pm}(m)$, and let $\tilde{f}_B(\Omega_p^{\pm}) = f_B(y^{\pm}(\Omega_p^{\pm}))$. Then, (i) $\nabla^2_{\Omega_p^{\pm}} \tilde{f}_B(\tilde{\psi}_p, 0)$ is diagonal with

$$\frac{\partial^2 \tilde{f}_B}{\partial \tilde{\psi}_{p,j}^2} (\tilde{\psi}_p, 0) = 0, \quad j = 1, 2; \quad \frac{\partial^2 \tilde{f}_B}{\partial r_{p,j}^{\pm 2}} (\tilde{\psi}_p, 0) = \lambda_j^{\pm}, \quad j = 1, 2, 3,$$
 (3.32)

 $\forall \tilde{\psi_p} \in B. \ Also, \ (ii) \ \frac{\partial \tilde{f_B}}{\partial \tilde{\psi}_{p,i}}(\Omega_p^\pm) = 0, \ j=1,2, \ \forall \Omega_p^\pm \in B \times I_\delta^3.$

3.2. Reduced equation and continuation of solutions

In this section, we outline the proofs of Propositions 2.3, 2.4, and 2.8. The main step is Lemma 3.11 below on the equivalence of the equation for critical points of $\overline{\mathcal{F}}$ for small |L| to a reduced equation for the "angular variables" parametrizing the L=0 critical set. In the case $U_-=\overline{G}$ the bifurcation equation is a discrete version of the equation for Oseen–Frank equilibria.

To set up Lemma 3.11, we parametrize a neighbourhood of the critical sets $C_0(\overline{\mathcal{F}_4}, U_+, U_-)$ of $\overline{\mathcal{F}_4}$ in $X(\overline{G})$. We let $U = U_+ \cup U_-$, and $U^c = G \setminus U$. U is assumed nonempty.

The set $X(\overline{G})$ is a product of the linear spaces Sym_0^3 , and we use the coordinates y_j (and w_j) of the previous section at each site: $Q(k) \in \operatorname{Sym}_0^3$, $k \in U \cup U^c$, is written as $Q(k) = \sum_{k \in U \cup U^c} \sum_{j \in \mathcal{J}} y_{k,j} \hat{Y}_j = \sum_{k \in U \cup U^c} \sum_{i=1}^5 w_{k,i} \hat{W}_i$, see (3.20). This defines an isomorphism (or chart) $\overline{\mathcal{B}}^w$: $(\operatorname{Sym}_0^3)^{|U|+|U^c|} \to \mathbb{R}^{5(|U|+|U^c|)}$, where $(\overline{\mathcal{B}}^w(Q))(k) = w(k) := [w_{k,1}, \dots, w_{k,5}]^T$. (An alternative notation is $\overline{\mathcal{B}}^y$.) The Riemannian metric on $\mathbb{R}^{5(|U|+|U^c|)}$ is the one induced by the standard Euclidean inner product, as in subsection 3.2. This metric is invariant under multiplication by the 5×5 matrices T_{A_k} , $T_{A_k} \in SO(3)$, applied (independently) at each site $T_{A_k} \in SO(3)$.

Also, the $C_0(\overline{\mathcal{F}_4}, U_+, U_-)$ of $\overline{\mathcal{F}_4}$ in $X(\overline{G})$ are products of projective planes, and their neighbourhood can be described using products of the coordinate systems of the previous section at the sites of U. The tangential directions at each site of U parametrize the critical sets.

Lemma 3.10. Let U_+ , U_- be disjoint subsets of \overline{G} with nonzero union. Then the critical set $C_0(\overline{\mathcal{F}}_4, U_+, U_-)$ of $\overline{\mathcal{F}}_4$ is an embedded submanifold of $X(\overline{G})$ and is diffeomorphic to $(\mathbb{R}P^2)^{|U|}$.

The proof follows by defining a map $\tilde{\Gamma}: (\mathbb{R}P^2)^{|U|} \to X(\overline{G})$ that is an embedding and an immersion, see [26]. Consider first the case where U_+, U_-, U^c are nonempty. We let

$$\tilde{\Gamma}: (\mathbb{R}P^2)^{|U_+|} \times (\mathbb{R}P^2)^{|U_-|} \to \mathbb{R}^{5|U_+|} \times \mathbb{R}^{5|U_-|} \times \mathbb{R}^{5|U^c|}, \tag{3.33}$$

by

$$\tilde{\Gamma}_{k}(m_{+}, m_{-}) = \begin{cases}
\tilde{\Gamma}_{-}(m_{+,k}), & k \in U_{+}, \\
\tilde{\Gamma}_{+}(m_{-,k}), & k \in U_{-}, \\
0, & k \in U^{c},
\end{cases}$$
(3.34)

where $m_{\pm} = \{m_{\pm,k}\}_{k \in U_{\pm}}$, and $\tilde{\Gamma}_{\pm}$ is as in (3.23). In the case where one of U_{+}, U_{-}, U^{c} is empty we delete the corresponding line from (3.34).

Assume that $U_+,\ U_-,\ U^c$ are nonempty. We then define a tubular neighbourhood $\mathcal T$ of the sets $\tilde{\Gamma}(\mathcal{C}_0(\overline{\mathcal{F}}_4, U_+, U_-))$ in $\mathbb{R}^{5|G|}$ as the union over $\mathbf{p} \in \mathcal{K}^{|U|}$ of the images of the maps $\mathbf{y_p}: \tilde{\mathcal{U}}_\mathbf{p} \times I_\delta^{3|U|} \times I_\delta^{5|U^c|} \to \mathbb{R}^{5(|U|+|U^c|)}$ with components

$$\mathbf{y}_{k,\mathbf{p}}(\tilde{\psi}_{\mathbf{p}}, r_{\mathbf{p}}, q_{\mathbf{p}}) = \begin{cases} \tilde{\Gamma}_{+}(\tilde{\psi}_{p_{k}}) + \sum_{i=1}^{3} r_{p_{k},i} \hat{N}_{p_{k},i}^{+}(\tilde{\psi}_{p_{k}}), & k \in U_{+}, \\ \tilde{\Gamma}_{-}(\tilde{\psi}_{p_{k}}) + \sum_{i=1}^{3} r_{p_{k},i} \hat{N}_{p_{k},i}^{-}(\tilde{\psi}_{p_{k}}), & k \in U_{-}, \\ q_{p_{k}}, & k \in U^{c}, \end{cases}$$
(3.35)

with $\delta > 0$, $r_{p_k,i} \in I_{\delta}$, for all $k \in U$, $p_k \in \mathcal{K}$, i = 1, 2, 3, and $q_{p_k} \in I_{\delta}^5$, for all $k \in U^c$. The $\hat{N}_{p_k,i}^{\pm}(\tilde{\psi}_{p_j})$, $\tilde{\psi}_{p_k} \in \tilde{\mathcal{U}}_{p_k}, p_k \in \mathcal{K}, k \in U$, are the normal vectors defined in the previous section. They are therefore eigenvectors of the Hessian of f_B with respect to the variables w(k) at $\tilde{f}_{\pm}(\tilde{\psi}_{p_k})$, for all $k \in U$. By Remark 3.8 the transition function between r_{p_k} , $r_{p'_k}$ is the identity, for any p_k , $p'_k \in \mathcal{K}$ with $\tilde{\mathcal{U}}_{p_k} \cap \tilde{\mathcal{U}}_{p'_k} \neq \emptyset$. Also $q_{p_k} = \{q_{p_k,i}\}_{i=1}^5 = \{w_{k,i}\}_{i=1}^5$, i.e. "cartesian coordinates" w_i , see (3.20), at each site of U^c . Transition functions for these components are the identity.

By Remark 3.7, expressions (3.35) with $\delta > 0$ sufficiently small define implicitly local coordinates for \mathcal{T} , in particular, \mathcal{T} is a union of neighbourhoods of $\tilde{\Gamma}(\tilde{\mathcal{U}}_p)$, where we have the "polar-cartesian" coordinates

$$\tilde{\psi}_{p_k} \in \tilde{\mathcal{U}}_{p_k}, \quad r_{p_k} \in I_{\delta}^3, \quad k \in U, \quad p_k \in \mathcal{K},$$
 (3.36)

$$q_{p_k} \in I_{\delta}^5, \quad k \in U^c. \tag{3.37}$$

In the case where one of U_j is empty, we delete the first (j = +) or second (j = -) line of (3.35), and (3.36). In the case where U^c is empty we delete the last line of (3.35), and (3.37).

We consider critical points of $\overline{\mathcal{F}}$ in the neighbourhood \mathcal{T} of the L=0 nontrivial critical sets. Consider first the case where U^c is nonempty. We let

$$g_{\mathbf{p},i}(k) = \frac{\partial \overline{\mathcal{F}}}{\partial \tilde{\psi}_{p_k,i}}, \quad i = 1, 2, \quad k \in U,$$
 (3.38)

$$h_{\mathbf{p},i}(k) = \frac{\partial \overline{\mathcal{F}}}{\partial r_{p_k,i}}, \quad i = 1, 2, 3, \quad k \in U,$$
 (3.39)

$$w_{\mathbf{p},i}(k) = \frac{\partial \overline{\mathcal{F}}}{\partial q_{p_k,i}}, \qquad i = 1, \dots, 5, \quad k \in U^c.$$
 (3.40)

These are the components of the derivative $D\overline{\mathcal{F}}$ in local coordinates $\tilde{\psi}_{\mathbf{p}}$, $r_{\mathbf{p}}$, $q_{\mathbf{p}}$, $\mathbf{p} \in \mathcal{K}^{|U|}$. Denoting the corresponding vectors by $g_{\mathbf{p}} \in \mathbb{R}^{2|U|}$, $h_{\mathbf{p}} \in \mathbb{R}^{3|U|}$, $w_{\mathbf{p}} \in \mathbb{R}^{5|U^c|}$, and letting $z_{\mathbf{p}} = 0$ $[r_{\mathbf{p}}, q_{\mathbf{p}}] \in I_{\delta}^{3|U|} \times I_{\delta}^{5|U^c|}$, we also define

$$F_{\tilde{\psi_{\mathbf{p}}}}\left(\tilde{\psi}_{\mathbf{p}},z_{\mathbf{p}},L\right)=g_{\mathbf{p}}(\tilde{\psi}_{\mathbf{p}},z_{\mathbf{p}},L),\quad F_{z_{\mathbf{p}}}(\tilde{\psi}_{\mathbf{p}},z_{\mathbf{p}},L)=\left[h_{\mathbf{p}}(\tilde{\psi}_{\mathbf{p}},z_{\mathbf{p}},L),w_{\mathbf{p}}(\tilde{\psi}_{\mathbf{p}},z_{\mathbf{p}},L)\right]. \tag{3.41}$$

Then critical points of $\overline{\mathcal{F}}$ in the vicinity of $\mathcal{C}_0(\overline{\mathcal{F}}_4, U_+, U_-) \cap \tilde{\mathcal{U}}_{\mathbf{p}}$ are solutions of

$$F_{\psi_{\mathbf{p}}}(\tilde{\psi}_{\mathbf{p}}, z_{\mathbf{p}}, L) = 0, \quad F_{z_{\mathbf{p}}}(\tilde{\psi}_{\mathbf{p}}, z_{\mathbf{p}}, L) = 0. \tag{3.42}$$

This follows from the fact that the polar-cartesian coordinate system is nonsingular in the neighbourhood of the sets $C_0(\overline{\mathcal{F}}_4, U_+, U_-) \cap \tilde{\mathcal{U}}_{\mathbf{p}}$.

The notation above also applies to the case where one of U_1 or U_2 is empty. In the case where U^c is empty, the $q_{\bf p}$, and $w_{\bf p}$ are not defined, and (3.40) is deleted. Also we use (3.41), (3.42) with $z_{\bf p} = r_{\bf p} \in I_{\delta}^{3|U|}$.

Lemma 3.11. Let $\overline{\mathcal{F}} = L\overline{\mathcal{F}}_2 + \overline{\mathcal{F}}_4$ be defined in a tubular neighborhood \mathcal{T} of $C_0(\overline{\mathcal{F}}_4, U_+, U_-)$ as above. (i) There exists $L_0 > 0$ such that for every $p \in \mathcal{K}^{|U|}$, $\tilde{\psi}_p \in \tilde{\mathcal{U}}_p$, and $L \in (-L_0, L_0)$ there exists a unique $\zeta_p(\tilde{\psi}_p, L) \in I_\delta^{3|U|} \times I_\delta^{5|U^c|}$ satisfying

$$F_{z_p}(\tilde{\psi}_p, \zeta_p(\tilde{\psi}_p, L), L) = 0, \tag{3.43}$$

and $\zeta_p(\tilde{\psi}_p, 0) = z_{p,0} = [0,0]$. The solution $\zeta_p(\tilde{\psi}_p, L)$ is real analytic in $\tilde{\psi}_p$, $\forall \tilde{\psi}_p \in \tilde{\mathcal{U}}_p$, and in L, $\forall L \in (-L_0, L_0)$. (ii) For $L \in (-L_0, L_0)$, solutions of the first equation of (3.42) are of the form $\tilde{\psi}_p = \chi$, $z_p = \zeta_p(\chi)$, with $\zeta_p(\cdot)$ as in (i), and χ solutions of the equation

$$\mathbf{g}_{\mathbf{p}}(\chi, L) = 0, \quad \chi \in \tilde{\mathcal{U}}_{\mathbf{p}},$$
 (3.44)

where

$$\mathbf{g}_{\mathbf{p}}(\tilde{\psi}_{p}, L) = D_{\tilde{\psi}_{p}}\mathcal{G}(\tilde{\psi}_{p}, L), \quad \mathcal{G}(\tilde{\psi}_{p}, L) := \overline{\mathcal{F}}(\tilde{\psi}_{p}, \zeta_{p}(\tilde{\psi}_{p}, L), L), \tag{3.45}$$

 $\forall \tilde{\psi}_{p} \in \tilde{\mathcal{U}}_{p}$, i.e. \mathcal{G} is the restriction of $\overline{\mathcal{F}}$ to the graph of ζ_{p} , $\forall \tilde{\psi}_{p} \in \tilde{\mathcal{U}}_{p}$, $p \in \mathcal{K}^{|U|}$. (iii) Let $L \in (-L_{0}, L_{0})$, then (i), (ii) define ζ , \mathbf{g} , \mathcal{G} globally on $\mathcal{M} = (\mathbb{R}P^{2})^{|U|}$ by $\zeta|_{\mathcal{U}_{p}} = \zeta_{p}$, $\mathbf{g}|_{\mathcal{U}_{p}} = \mathbf{g}_{p}$, $\mathcal{G}|_{\mathcal{U}_{p}} = \mathcal{G}_{p}$, for all $\mathbf{p} \in \mathcal{K}^{|U|}$.

Lemma 3.11 reduces the problem of finding equilibria of the Landau–de Gennes system for L sufficiently near the origin to that of finding critical points of \mathcal{G} on $(\mathbb{R}P^2)^{|U|}$. The proof is based on the implicit function theorem [5] and is omitted as it is exactly as in the case with boundary, see Lemma 4.2, [26]. The system of coordinates defined above using the symmetry of f_B makes the computation of the derivative straightforward.

A consequence of Lemma 3.11 is that given a solution $\chi \in \tilde{\mathcal{U}}_{\mathbf{p}}$ of the reduced equation, the components $r_{\mathbf{p}}$, $q_{\mathbf{p}}$ of the equilibrium are given by $\zeta_{\mathbf{p}}(\chi, L)$. Necessary continuation conditions are obtained by the reduced equation at L=0.

Proof of Proposition 2.3 By Lemma 3.11, for L sufficiently near 0 it is sufficient to study solutions of the reduced equation (3.45)

$$\mathbf{g}_{\mathbf{p}}(\tilde{\psi}_{\mathbf{p}},L) = D_{\tilde{\psi}_{\mathbf{p}}}\overline{\mathcal{F}}(\tilde{\psi}_{\mathbf{p}},\zeta_{\mathbf{p}}(\tilde{\psi}_{\mathbf{p}},L),L) = D_{1}\overline{\mathcal{F}}(\tilde{\psi}_{\mathbf{p}},\zeta_{\mathbf{p}}(\tilde{\psi}_{\mathbf{p}},L),L) = 0,$$

for some $\mathbf{p} \in \mathcal{K}^{|U|}$. The functions $\zeta_{\mathbf{p}}$ and $\overline{\mathcal{F}}$ are real analytic and we can expand $\mathbf{g}_{\mathbf{p}}$ in powers of L as

$$\mathbf{g}_{\mathbf{p}}(\psi, L) = \sum_{k=1}^{\infty} L^{k} \mathbf{g}_{\mathbf{p}, k}(\psi), \quad |L| < L_{0}.$$
 (3.46)

Moreover $D_1\overline{\mathcal{F}}_4$ vanishes identically by Lemma 3.9 (ii). The lowest order term in (3.46) is then

$$\mathbf{g}_{\mathbf{p},1}(\tilde{\psi}_{\mathbf{p}}) = D_{\tilde{\psi}_{\mathbf{p}}}\overline{\mathcal{F}}_{2}(\tilde{\psi}_{\mathbf{p}}, \zeta_{\mathbf{p}}(\tilde{\psi}_{\mathbf{p}}, 0)) = D_{\tilde{\psi}_{\mathbf{p}}}\overline{\mathcal{F}}_{2}(\tilde{\psi}_{\mathbf{p}}, 0). \tag{3.47}$$

By the hypothesis of Proposition 2.3, and Lemma 3.11, we have a branch $\tilde{\Theta}(L)$, $L \in [0, \epsilon_0)$, $\epsilon_0 \le L_0$, of solutions of $\mathbf{g}_{\mathbf{p}}(\tilde{\Theta}(L), L) = 0$, and therefore

$$L^{-1}\mathbf{g}_{\mathbf{n}}(\tilde{\Theta}(L), L) = 0, \quad \forall L \in (0, \epsilon_0). \tag{3.48}$$

Taking the limit $L \to 0^+$, and using (3.46), (3.47), we have that $\Theta = \tilde{\Theta}(0)$ satisfies

$$\mathbf{g}_{\mathbf{p},1}(\Theta) = D_{\tilde{\psi}_{\mathbf{p}}} \overline{\mathcal{F}}_{2}(\Theta,0) = 0, \tag{3.49}$$

as stated.

The main feature of the continuation problem for graphs without boundary is that the reduced equations for $\overline{\mathcal{F}}$ have a global SO(3) symmetry. This implies that solutions of the reduced equations are in general not isolated points.

To see how the continuation argument is modified, fix $A \in SO(3)$ and define $\Psi_A^d : (\operatorname{Sym}_0^3)^{|\overline{G}|} \to (\operatorname{Sym}_0^3)^{|\overline{G}|}$ by

$$\Psi_A^d(\overline{Q})(m) = \Psi_A(\overline{Q}(m)), \quad m \in \overline{G}. \tag{3.50}$$

By (2.6) and Lemmas 3.2, 3.4 $\overline{\mathcal{F}}$ is invariant under Ψ^d_A , for all $A \in SO(3)$ and L real. Also define $T^d_A : \mathbb{R}^{5|\overline{G}|} \to \mathbb{R}^{5|\overline{G}|}$ by

$$(T_A^d y)(m) = T_A y(m), \quad m \in \overline{G}. \tag{3.51}$$

The manifold \mathcal{M} is invariant under T_A^d , $\forall A \in SO(3)$. Also define $T^d: SO(3) \times \mathbb{R}^{5|\overline{G}|} \to \mathbb{R}^{5|\overline{G}|}$ by $T^d(A,y) = T^dy$. We use the polar-cartesian coordinates above in the neighbourhood of $\mathcal{M} \subset \mathbb{R}^{5|\overline{G}|}$, and denote the angular, and polar components of T_A^d in the neighbourhood of some $\tilde{\mathcal{U}}_{\mathbf{p}}$ by $\mathcal{R}_{A,\mathbf{p}}^d(\tilde{\psi}_{\mathbf{p}},z_{\mathbf{p}})$, respectively. By Remark 3.8, $\mathcal{R}_{A,\mathbf{p}}^d(\tilde{\psi}_{\mathbf{p}},z_{\mathbf{p}})$ coincides with the restriction of T_A^d to \mathcal{M} , and depends only on the angular part. We thus write $\mathcal{R}_{A,\mathbf{p}}^d(\tilde{\psi}_{\mathbf{p}},z_{\mathbf{p}}) = \mathcal{R}_{A,\mathbf{p}}^d(\tilde{\psi}_{\mathbf{p}})$. Also let \mathcal{R}_A^d denote the restriction of T_A^d to \mathcal{M} , and denote the corresponding action of SO(3) on \mathcal{M} by \mathcal{R}^d .

Lemma 3.12. Consider the functions ζ , \mathbf{g} , and \mathcal{G} of Lemma 3.11, with $|L| < L_0$. Then (i) ζ is equivariant under \mathcal{R}_A^d , see (3.52), $\forall A \in SO(3)$, (ii) \mathcal{G} is invariant under \mathcal{R}_A^d , $\forall A \in SO(3)$, and (iii) critical points of \mathcal{G} belong to compact embedded submanifolds of $\mathcal{M} \approx (\mathbb{R}P^2)^{|U|}$.

Proof. To see (i) fix $L \in (-\epsilon_0, \epsilon_0)$ and let $\zeta_{\mathbf{p}}(\tilde{\psi}_{\mathbf{p}}) = \zeta_{\mathbf{p}}(\tilde{\psi}_{\mathbf{p}}, L)$, $\mathbf{p} \in \mathcal{K}^{|U|}$. Assume first that A is such that T_A^d maps a critical point $m \in \tilde{\mathcal{U}}_{\mathbf{p}}$ to a point in the same domain. It suffices to show the local version of equivariance, namely

$$Z_{A,\mathbf{p}}^{d}(\tilde{\psi}_{\mathbf{p}},\zeta_{\mathbf{p}}(\tilde{\psi}_{\mathbf{p}})) = \zeta_{\mathbf{p}}(\mathcal{R}_{A,\mathbf{p}}^{d}(\tilde{\psi}_{\mathbf{p}})). \tag{3.52}$$

Note that $z = \zeta(\mathcal{R}^d_{A,\mathbf{p}}(\tilde{\psi}_{\mathbf{p}}))$ is a solution of (3.43). Invariance of $\overline{\mathcal{F}}$ under \mathcal{R}^d_A implies that the image of a critical point of $\overline{\mathcal{F}}$ under \mathcal{R}^d_A is also a critical point of $\overline{\mathcal{F}}$, therefore $z = Z^d_{A,\mathbf{p}}(\tilde{\psi}_{\mathbf{p}})$ also satisfies (3.43). By Lemma 3.11 the solution of (3.43) is unique and the two sides of (3.52) must coincide. In the case of arbitrary $A \in SO(3)$ we write A as a finite product of elements of SO(3) satisfying the above assumption.

To show (ii) we similarly work with compositions of T_A^d , restricted to \mathcal{M} , that map a subset of $\tilde{\mathcal{U}}_{\mathbf{p}}$ to a subset of $\tilde{\mathcal{U}}_{\mathbf{p}}$. We have

$$\widetilde{\mathcal{G}}(\mathcal{R}^d_A(\tilde{\psi}_{\mathbf{p}})) = \overline{\mathcal{F}}(\mathcal{R}^d_A(\tilde{\psi}_{\mathbf{p}}), \zeta_{\mathbf{p}}(\mathcal{R}^d_A(\tilde{\psi}_{\mathbf{p}})) = \overline{\mathcal{F}}(\mathcal{R}^d_A(\tilde{\psi}_{\mathbf{p}}), Z^d_{\mathbf{p}}(\psi_{\mathbf{p}}, \zeta_{\mathbf{p}}(\tilde{\psi}_{\mathbf{p}})) = \overline{\mathcal{F}}(\tilde{\psi}_{\mathbf{p}}, \zeta_{\mathbf{p}}(\tilde{\psi}_{\mathbf{p}})),$$

using (i) and the invariance of $\overline{\mathcal{F}}$ under T_A^d . Thus $\mathcal{G}(\mathcal{R}_A^d(\tilde{\psi}_{\mathbf{p}})) = \mathcal{G}(\tilde{\psi}_{\mathbf{p}})$.

To see (iii), we use a similar strategy using local coordinates in $(\mathbb{R}P^2)^{|U|}$ and a standard argument to see that the critical points $\tilde{\mathcal{G}}$ are mapped to critical points under \mathcal{R}_A^d Furthermore \mathcal{R}_A^d is a smooth SO(3)-action on $\mathcal{M} \approx (\mathbb{R}P^2)^{|U|}$. Since SO(3) is compact, the orbit of every point $x \in \mathcal{M}$ under this action is a compact embedded submanifold $\mathcal{O}_{SO(3)}(x)$ of \mathcal{M} , see [18].

Proof of Lemma 2.2 Let $L_0 > 0$ be as in Lemma 3.11. Critical sets of $\overline{\mathcal{F}}$, $|L| < L_0$, are graphs of critical points of \mathcal{G} under the map ζ of Lemma 3.11. This map embedds $(\mathbb{R}P^2)^{|U|}$ to $\mathbb{R}^{5|\overline{G}|}$. Its restriction to critical sets of \mathcal{G} are also embeddings and are critical sets of \mathcal{G} . By Lemma 3.11, all critical set of \mathcal{G} , $|L| < L_0$, are of that form.

Proof of Proposition 2.4 s By Lemma 3.11, to find critical points of $\overline{\mathcal{F}}$, $|L| < L_0$, it suffices to find critical points of the functional $\mathcal{E}(\tilde{\psi}, L) = \overline{\mathcal{F}}_2(\tilde{\psi}, \zeta(\tilde{\psi}, L))$, $|L| < L_0$, $\tilde{\psi} \in (\mathbb{R}P^2)^{|U|}$. The statement follows from the assumption by using normal coordinates around each manifold of critical points and the implicit function theorem argument of Lemma 3.11.

The manifolds of critical points of the reduced energy \mathcal{G} on $\mathcal{M} \approx (\mathbb{R}P^2)^d$ can be classified by classifying the topology of orbits of the diagonal action \mathcal{R}^d of SO(3) on \mathcal{M} , i.e. T^d of (3.51), restricted to \mathcal{M} . The basic fact from the theory of Lie group actions is that the orbit $\mathcal{O}(x)$ of $x \in \mathcal{M}$ under the action of SO(3) is the manifold $SO(3)/SO(3)_x$, where $SO(3)_x$ is the isotropy subgroup of x under the action, see the theorem of section 5.15 of [16]. In what follows we classify the isotropy subgroups.

By the definition of the action, the isotropy subgroup $SO(3)_x$ under \mathbb{R}^d is the set of all $R \in SO(3)$ satisfying

$$R \hat{n} = \pm \hat{n}, \quad \forall \hat{n} \in \mathcal{V}(x).$$
 (3.53)

The set of such matrices is a subgroup of SO(3).

By (3.53) The action only affects the directions of the Q-tensors on Σ_{\pm} , thus a configuration on \mathcal{M} is determined by the directions $\{\hat{n}_j, -\hat{n}_j\}$, where j is either in U_- or U_+ . Denote by $\mathcal{V}(x)$, $x = (x_1, \ldots, x_d) \in (\mathbb{R}P^2)^d$, the set distinct points of $\mathbb{R}P^2$ in $\{x_1, \ldots, x_d\}$. Let $\tilde{d}(x)$ denote the number of values of $x \in (\mathbb{R}P^2)^d$. Clearly $1 \le \tilde{d}(x) \le d$, $\forall x \in (\mathbb{R}P^2)^d$. By (3.53) the isotropy subgroup of x depends on $\mathcal{V}(x)$. For $l, l' \in \mathcal{V}(x)$ we use expressions $l \perp l', l^\perp$, etc., to denote orthogonality, orthogonal complement, etc., of directions in \mathbb{R}^3 with respect to the Euclidean inner product.

In the case $\tilde{d}(x) = 1$ we have $\mathcal{O}_{SO(3)}(x) \approx \mathbb{R}P^2$ by Lemma 3.3. The isotropy subgroup below for that case describes the projective plane as a quotient of SO(3) by the isotropy subgroup of points in the diagonal of \mathcal{M} . The case where $U_{\pm} = \overline{G}$, $U_{\mp} = \emptyset$ and $\tilde{d} = 1$ corresponds to the constant critical points of $\overline{\mathcal{F}}$. For abelian group actions on products the orbits of points in the diagonal are diffeomorphic to all orbits. This is not necessarily the case for nonabelian group actions.

Let

$$R_{\phi} = \begin{bmatrix} \cos \phi & -\sin \phi & 0 \\ \sin \phi & \cos \phi & 0 \\ 0 & 0 & 1 \end{bmatrix}, \quad A_{-} = \begin{bmatrix} -1 & 0 & 0 \\ 0 & 1 & 0 \\ 0 & 0 & 1 \end{bmatrix}. \tag{3.54}$$

Note that $(A_-)^{-1} = A_-$, $R_\phi^{-1} = R_{-\phi}$, $(A_-R_\phi)^{-1} = R_{-\phi}A_-$, for all $\phi \in [0, 2\pi)$ also the matrices A_- , R_π , A_-R_π describe rotations by π around the vectors \hat{e}_1 , \hat{e}_3 , \hat{e}_2 respectively, and $\{I, A_-, R_\pi, A_-R_\pi\}$, $I = R_0$, form an abelian group that contains the subgroups $\{I, A_-\}$, $\{I, R_\pi\}$, $\{I, A_-R_\pi\}$, and the trivial group $\{I\}$.

Let S_1 , S_2 be subgroups of SO(3). We say that S_1 , S_2 are isomorphic (under conjugacy) and we write $S_1 \sim S_2$ if there exists an $A \in SO(3)$ such that the map $ad_A : S_1 \to S_2$, defined by $ad_A(g_1) = A^{-1}g_1A$, $g_1 \in S_1$, is a group isomorphism. Note that the isotropy subgroups of $x, y \in (\mathbb{R}P^2)^d$ with $x_j = Ay_j$, $A \in SO(3)$, $j = 1, \ldots, d$, are isomorphic since by (3.53), $R \in SO(3)_x$ if and only if $A^{-1}RA \in SO(3)_y$.

Proposition 3.13. Let $x \in \mathcal{M}$, then the isotropy group $SO(3)_x$ under \mathbb{R}^d is as follows.

- (i) If d(x) = 1 then $SO(3)_x$ is isomorphic to the set S_r of all R_{ϕ} , $R_{\phi}A_-$, A_-R_{ϕ} , $\phi \in [0, 2\pi)$.
- (ii) Let d(x) = 2 and $\mathcal{V}(x) = \{l_1, l_2\}$ If (α) $l_1 \not\perp l_2$ then $SO(3)_x$ is isomorphic to the set $\{I, R_{\pi}A_{-}\}$. If (β) $l_1 \perp l_2$ then $SO(3)_x$ is isomorphic to the set $\{I, A_{-}, R_{\pi}, R_{\pi}A_{-}\}$.
- (iii) Let d=3. If the elements of V(x) lie on the same plane then $SO(3)_x$ is isomorphic to the set $\{I, R_{\pi}A_{-}\}$. If the elements $l_1, l_2, l_3 \ V(x)$ are linearly independent we have four subcases: $(\alpha) \ l_i \ \not\perp \ l_j$, $\forall i, j \in \{1, 2, 3\}$, then $SO(3)_x$ is $\{I\}$; $(\beta) \ l_1 \ \perp \ l_2$ with $l_3 \ \not\perp \ l_1$ and $l_3 \ \not\perp \ l_2$ (up to renumbering), then $SO(3)_x$ is $\{I\}$; $(\gamma) \ l_2, \ l_3 \in l_1^{\perp}$ and $l_2 \ \not\perp \ l_3$ (up to renumbering), then $SO(3)_x$ is isomorphic to the set $\{I, R_{\pi}\}$; $(\delta) \ l_i \ \perp \ l_j, \ \forall i, j \in \{1, 2, 3\}$, $SO(3)_x$ is isomorphic to the set $\{I, A_{-}, R_{\pi}, R_{\pi}A_{-}\}$.
- (iv) Let $d \ge 4$. If all the elements of $\mathcal{V}(x)$ lie on the same plane then $SO(3)_x$ is isomorphic to the set $\{I, R_{\pi}A_{-}\}$. If the elements of $\mathcal{V}(x)$ are not on the same plane and there is no pair of $l_1, l_2 \in \mathcal{V}(x)$ satisfying $l_1 \perp l_2$, then $SO(3)_x$ is $\{I\}$. If there exists a pair of vectors $l_1, l_2 \in \mathcal{V}(x)$ satisfying $l_1 \perp l_2$ and either $\mathcal{V} \setminus \{l_1\} \in l_2^{\perp}$ or $\mathcal{V} \setminus \{l_2\} \in l_1^{\perp}$ then $SO(3)_x$ is isomorphic to $\{I, R_{\pi}\}$, otherwise $SO(3)_x$ is $\{I\}$.

Proof. Note that the isotropy subgroups of $x, y \in (\mathbb{R}P^2)^d$ with $x_j = \tilde{R}y_j$, $\tilde{R} \in SO(3)$, j = 1, ..., d, are isomorphic since by (3.53) $R \in SO(3)_x$ if and only if $\tilde{R}^{-1}R\tilde{R} \in SO(3)_y$. To compute $SO(3)_x$ up to isomorphism we may rotate the elements of $\mathcal{V}(x)$ to some standard configurations.

- (i) The line $l \in \mathcal{V}(\S)$ can be rotated to the direction of \hat{e}_3 by two rotation matrices R_1, R_2 . Solutions of (3.53) with $\hat{n} = \hat{e}_3$ are rotation matrices whose third column is $\pm \hat{e}_3$. In the case where the third column is \hat{e}_3 , the solutions are the matrices R_{ϕ} , $\phi \in [0, 2\pi)$. In the case where the third column is $-\hat{e}_3$, the first 2×2 block is a rotation matrix with determinant -1. The resulting rotation matrices are of the form $R_{\phi}A_-, A_-R_{\phi}, \phi \in [0, 2\pi)$.
- (ii) Let $V(x) = \{l_1, l_2\}$. Rotate l_1 to the direction of \hat{e}_3 , then rotate around the axis of \hat{e}_3 to obtain the directions of two noncolinear vectors \hat{e}_3 , \tilde{n}_2 on the plane span $\{\hat{e}_3, \hat{e}_1\}$. If $\tilde{n}_2 \neq \pm \hat{e}_1$, case (α) , then (3.53) with $\hat{n} = \tilde{n}_2$ has solutions R = I, $R_{\pi}A_{-} = A_{-}R_{\pi} = (R_{\pi}A_{-})^{-1}$. These matrices also leave the axis of \hat{e}_3 invariant. If $\tilde{n}_2 = \pm \hat{e}_1$, case (β) , then (3.53) with $\hat{n} = \tilde{n}_2$ has solutions R = I, A_{-} , $R_{\pi}A_{-}$. These matrices also leave the directions of \hat{e}_i , j = 1, 2, 3, invariant.
- (iii) Let $V(x) = \{l_1, l_2, l_3\}$. We apply a rotation to transform the first two directions to the directions of the vectors \hat{e}_3 , \tilde{n}_2 on the plane span $\{\hat{e}_3, \hat{e}_1\}$ as in (ii). We also obtain a third direction along a vector \tilde{n}_3 .

If the three directions of V(x) are on the same plane then $\tilde{n}_3 \in \text{span}\{\hat{e}_3, \tilde{n}_2\}$, and we have case (α) of (ii) for two of the directions. The third direction belongs to the same plane, and we have the isotropy subgroup of (ii) (α) .

In the case where $\{l_1, l_2, l_3\}$ are linearly independent, subcase (α) , we have $\tilde{n}_3 \notin \text{span}\{\hat{e}_3, \hat{e}_1\}$, and $\tilde{n}_3 \neq \hat{e}_3$, then $\tilde{n}_3 = [x_1, x_2, x_3]$, with $x_2, x_3 \neq 0$. Also the isotropy subgroup is a subset of that of (ii), case (α) since $\hat{e}_3 \neq \tilde{n}_2$. The equation $R_{\pi}A_{-}\tilde{n}_3 = \pm \tilde{n}_3$ implies $x_2 = x_2$, $-x_3 = x_3$ or $x_2 = -x_2$, $x_3 = x_3$, and there are no solutions with both x_2, x_3 nonvanishing.

In subcase (β) we may assume that $l_1 \perp l_2$, and $\tilde{n}_2 = \hat{e}_1$. Then l_3 is mapped to $\tilde{n}_3 = [x_1, x_2, x_3]$, with $x_1, x_2, x_3 \neq 0$ by the assumptions. The isotropy subgroup is a subset of the set of (ii), case (β) since $l_1 \perp l_2$. By the argument of subcase (iii) (α) the direction of \tilde{n}_3 is not invariant under A_- , R_π ,

 $A_{-}R_{\pi}$, they all leave one component invariant and change the sign of the other two, and we cannot have solutions with all components nonzero.

In subcase (γ) , the transformed vectors satisfy $\tilde{n}_2 = \hat{e}_1$, $\tilde{n}_3 \in \hat{e}_3$, $\tilde{n}_2 \neq \tilde{n}_3$. Moreover $\tilde{n}_3 = [x_1, x_2, 0]$ with $x_1, x_2 \neq 0$. The isotropy subgroup is a subset of the group of (ii), case (β) . The direction of \tilde{n}_3 is invariant under R_{π} , but not under A_{-} or $A_{-}R_{\pi}$, thus $SO(3)_x$ is isomorphic to $\{I, R_{\pi}\}$.

In the subcase (δ) the transformed directions are \hat{e}_j , j=1,2,3, and we have the isotropy group of (ii), case (β) since the additional direction of \hat{e}_3 is also invariant under its transformations. The above cover all possible $\mathcal{V}(x)$ with three elements.

(iv) In the case where all directions of V(x) are on the same plane, we use the argument of (iii) to bring all directions to the plane of \hat{e}_3 , \hat{e}_1 . The isotropy subgroup is the same as the the one obtained for the d=3 coplanar case as the extra directions are also invariant under the T_-R_π .

If the directions of V(x) are not on the same plane we distinguish the cases where the none or at least one pair of orthogonal directions. In the first case we have three directions as in (iii), subcase (α) and the isotropy subgroup is trivial.

In the second case consider a pair of $l_1 \perp l_2 \in \mathcal{V}(x)$. We first consider the subcase where all other vectors are in l_j^{\perp} , $j \in \{1, 2\}$. Then we transform l_j to \hat{e}_3 and see that we have at least two other transformed vectors in \hat{e}^{\perp} that are as in (ii), subcase (γ). These directions are invariant under A_-R_{π} , and so are all other vectors in \hat{e}^{\perp} . Thus the isotropy subspace is $\{I, A_-R_{\pi}\}$. If on the contrary, there is at least one direction not in either l_1^{\perp} or l_2^{\perp} , we have three directions satisfying the assumptions of (ii), subcase (β), and the isotropy subgroup is trivial. The above cover all possible $\mathcal{V}(x)$ with at least four elements. \square

Since the vectors \hat{e}_j can be transformed to each other by a rotation the groups $\{I, A_-\}$, $\{I, R_\pi\}$, $\{I, A_-R_\pi\}$ are isomorphic. Thus the isotropy subgroups found are, up to isomorphism, the set S_r of (i), the abelian group of two elements $\{I, R_\pi\}$, the abelian group $\{I, A_-, R_\pi, A_-\}$, and the trivial subgroup $\{I\}$.

Proposition 2.7 on the connection between the reduced functionals appearing in the bifurcation equation and discretized Oseen–Frank functionals for the case without boundary follows from the computation of [26] for the case with boundary.

The main observation is that equation (3.49) for critical points of $\overline{\mathcal{F}}_2$, see (2.5), restricted to $C^0 = C^0(\overline{\mathcal{F}}_4, U_1, U_2)$ with $U_1 = \overline{G}$, $U_2 = \emptyset$ are critical points over configurations where the Q(m) have i, jth entry

$$\overline{Q}_{i,j}(m) = -3x_{-}(\hat{n}_{i}(m)\hat{n}_{j}(m) - \frac{1}{3}\delta_{i,j}), \quad \hat{n}(m) \in S^{2},$$
(3.55)

for all $m \in \overline{G}$. Denoting $\overline{\mathcal{F}}_2$ restricted to C^0 by $\overline{\mathcal{F}}_{2,r}$ and using (2.5) we have

$$\overline{\mathcal{F}}_{2,r}(\hat{n}) = -\frac{3x_{-}}{2} \sum_{k,m \in \overline{G}} c(k,m) (2 - 2(\hat{n}(k) \cdot \hat{n}(m))^{2}), \quad \hat{n} : \overline{G} \to S^{2},$$
(3.56)

with \cdot the standard inner product in \mathbb{R}^3 . Thus $\overline{\mathcal{F}}_{2,r}$ does not depend on the signs of the $\hat{n}(m)$, $m \in \overline{G}$, and is well-defined as a functional on maps from \overline{G} to $\mathbb{R}P^2$.

In contrast, the Oseen–Frank functional \mathcal{F}_{OF} of (2.3) can be discretized by

$$\overline{\mathcal{F}}_{OF}(\overline{\mathbf{n}}) := \frac{1}{2} \sum_{k,m \in \overline{G}} c(k,m) |\overline{\mathbf{n}}(k) - \overline{\mathbf{n}}(m)|^{2}$$

$$= \frac{1}{2} \sum_{k,m \in \overline{G}} c(n,m) (2 - 2(\overline{\mathbf{n}}(k) \cdot \overline{\mathbf{n}}(m))), \quad \overline{\mathbf{n}} : \overline{G} \to S^{2}. \tag{3.57}$$

This functional is not invariant under arbitrary changes of sign of $\overline{\mathbf{n}}$ at the different sites, see discussion in [26] comparing (3.56), (3.57).

The proof of Proposition 2.8 for the case without boundary is as in the case without boundary in [26] and is omitted.

4. Numerical integration of the gradient flow

We present results obtained by numerical integration of the gradient of the Landau–de Gennes energy in some simple geometries. We are interested in the regime of small L > 0, with $U_- = \overline{G}$ (case without boundary) and $U_- = G$ (case with boundary). The first effect sought is convergence to equilibria that are near-uniaxial. We also compare the time scales of approach to a near-uniaxial state and convergence to an equilibrium. A second effect we examine is the possibility of multiple attracting equilibria in the periodic chain.

4.1. Discrete geometries: boundary and initial conditions

For a set G of N sites, the Q-tensor Q(k) at site $k \in \{1, ..., N\}$ is described by its components $y_j(k)$, $j \in \{1, ..., 5\}$, defined in section 3. The gradient equations

$$\dot{Q} = -\nabla \mathcal{G}(Q),$$

 $\mathcal{G}(Q) = \mathcal{F}_{LG}(Q)$ (case without boundary), $\mathcal{G}(Q) = \overline{\mathcal{F}}_{LG}(Q; Q_b)$ (case with boundary), $\nabla = \nabla_Q$, have the general form

$$\dot{y}_{j}(k) = -L(\Delta y_{j})(k) - \frac{\partial f_{B}(Q(k))}{\partial y_{i}(k)}, \quad j \in \{1, \dots, 5\}, \quad k \in \{1, \dots, N\}.$$
(4.1)

The second term is the gradient of the onsite energy

$$f_B(Q(k)) = -\frac{a^2}{2} \operatorname{tr}(Q(k)^2) - \frac{b^2}{3} \operatorname{tr}(Q(k)^3) + \frac{c^2}{4} (\operatorname{tr}(Q(k)^2))^2, \tag{4.2}$$

$$tr(Q(k)^2) = y_1(k)^2 + y_2(k)^2 + y_3(k)^2 + y_5(k)^2 + y_6(k)^2,$$
(4.3)

$$\operatorname{tr}(Q^{3}(k)) = \frac{3}{\sqrt{6}} y_{2}(k)^{2} y_{5}(k) + \frac{3}{\sqrt{2}} y_{2}(k) y_{3}(k) y_{6}(k) + \frac{3}{2\sqrt{2}} (y_{3}(k)^{2} y_{1}(k) - y_{6}(k)^{2} y_{1}(k)) - \frac{3}{2\sqrt{6}} (y_{3}(k)^{2} y_{5}(k) + y_{6}(k)^{2} y_{5}(k)) - \frac{1}{\sqrt{6}} y_{5}(k)^{3} + \frac{3}{\sqrt{6}} y_{1}(k)^{2} y(k)_{5},$$

for all $k \in \{1, ..., N\}$, and has the same form at all interior sites.

The first term $(\Delta y_j)(k)$ at site k is the linear coupling to other sites and contains the information about the geometry of the set G.

Geometry A. Chain with two boundary points. In the case of a chain with nearest-neighbour interactions and boundary values y_L , $y_R \in \mathbb{R}^5$, e.g. setting $y(0) = y_L$, $y(N+1) = y_R$, we have

$$(\Delta y_i)(k) = y_i(k-1) + y_i(k+1) - 2y_i(k), \quad k \in \{2, \dots, N-1\},$$
(4.4)

$$(\Delta y_i)(1) = y_{L,i} + y_i(2) - 2y_i(1), \quad (\Delta y_i)(N) = y_i(N-1) + y_{R,i} - 2y_i(N), \tag{4.5}$$

with $y_L = \{y_{L,j}\}_{j=1}^5$, $y_R = \{y_{R,j}\}_{j=1}^5$, for all $j \in \{1, \dots, 5\}$.

Geometry B. Closed chain. In the case of a chain with nearest-neighbour interactions and periodic boundary conditions

$$(\Delta y_i)(k) = y_i(k-1) + y_i(k+1) - 2y_i(k), \quad k \in \{2, \dots, N-1\},$$
(4.6)

$$(\Delta y_i)(1) = y_i(N) + y_i(2) - 2y_i(1), \quad (\Delta y_i)(N) = y_i(N-1) + y_i(1) - 2y_i(N), \tag{4.7}$$

for all $j \in \{1, ..., 5\}$.

We integrate numerically the equations for the two systems with initial conditions that are not

Geometry A. In the case of the open chain, we choose uniaxial boundary conditions Q_L , Q_R

$$Q_j = -3x_-\left(\hat{n}(j) \otimes \hat{n}(j) - \frac{1}{3}I\right), \quad j = L, R,$$
 (4.8)

 x_{-} the negative solution of $-a^2 + 6c^2x + b^2x^2 = 0$. We use the values $b^2 = \sqrt{6}$, $a^2 = \frac{1}{2}$, $c^2 = \frac{2}{3}$, then $x_{-} = \frac{1}{\sqrt{6}}$.

The unit vectors $\hat{n}(L)$, $\hat{n}(R)$ are at an angle. The corresponding Q-tensors are obtained from the polar representation (3.24) of the vectors $\hat{n}(L)$, $\hat{n}(R)$, via (3.18).

The corresponding vectors y_L , y_R are obtained via (3.11)-(3.14), i.e. the respective Q_L , Q_R are as in (3.10) The initial condition at the interior points is chosen to be

$$y(k) = \frac{k}{N+1}(y_R - y_L), \quad k = 1, \dots, N.$$
 (4.9)

The interior values interpolate linearly between the boundary values, and are not generally uniaxial. In cases of boundary conditions expected to lead to more than one attracting equilibria, we use small perturbations of (4.9) that may lead to different asymptotic states.

Geometry B. In the closed chain we use uniaxial initial conditions of the form

$$Q(k) = s(k) \left(\hat{n}(k) \otimes \hat{n}(k) - \frac{1}{3}I \right), \quad k \in \{1, \dots, N\},$$

with different choices of the functions s, \hat{n} . The choice $s = -3x_{-}$ at all sites, x_{-} the negative solution of $-a^2 + 6c^2x + b^2x^2 = 0$, corresponds to an initial condition of uniaxial tensors on the manifold of minima

We use the values $b^2 = \sqrt{6}$, $a^2 = \frac{1}{2}$, $c^2 = \frac{2}{3}$, then $x_- = \frac{1}{\sqrt{6}}$.

Also, we consider

$$s(k) = \sigma((k-1)/N), \quad k \in \{1, \dots, N\},\$$

for σ smooth 1-periodic functions that oscillate around the value $-3x_-$, and

$$\hat{n}(k) = \hat{v}((k-1)/N), \quad k \in \{1, \dots, N\},\$$

where $\hat{v}: [0,1] \to S^2$ are smooth parameterized curves.

We are interested in two classes of curves \hat{v} , corresponding to initial conditions expected to converge to states that are discrete analogues of the two homotopy classes of $\mathbb{R}P^2$.

First, we consider closed curves that are continuous deformations of curves whose image is a subset of an open hemisphere, see e.g. Figure 1(a). The corresponding initial conditions are expected to converge to discrete analogues of homotopicaly trivial curves on $\mathbb{R}P^2$, i.e. curves that can be continuously deformed to point.

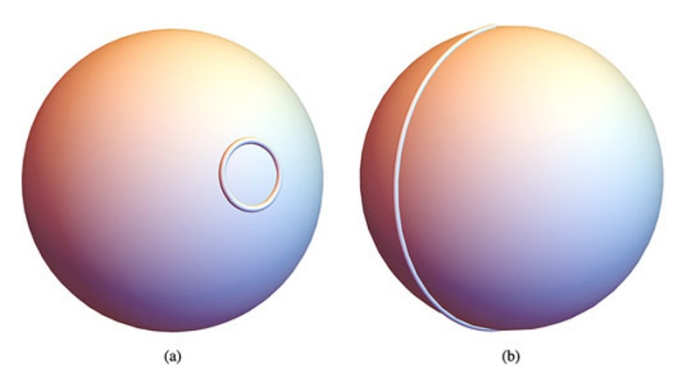


Figure 1. Examples of closed curves of the two homotopy classes of $\mathbb{R}P^2$, visualization using the 2-sphere. When antipodal points are identified, (a) depicts a homotopically trivial curve on the projective plane, while (b) depicts a homotopically non-trivial curve on the projective plane.

Also, we consider curves that are continuous deformations of curves that join any two antipodal points of S^2 , see e.g. Figure 1(b). The corresponding initial conditions are expected to converge to discrete analogues of homotopically nontrivial curves on $\mathbb{R}P^2$, i.e. curves that cannot be continuously deformed to a point.

An example of an initial condition expected to converge to a configuration that is a discrete analogue of a homotopicaly trivial curve in $\mathbb{R}P^2$ is

$$\phi(k) = \frac{\pi}{2} + \frac{1}{5}\cos\frac{2(k-1)\pi}{N}, \quad \theta(k) = \frac{\pi}{2} + \frac{1}{5}\sin\frac{2(k-1)\pi}{N}, \quad s(k) = \frac{3}{\sqrt{6}}; \tag{4.10}$$

k = 1, ..., N. The corresponding Q(k), and y(k) are obtained via (3.18), (3.11)-(3.14), (3.10). Figure 1(a) depicts the vectors \hat{n} of the curve defined by (4.10). This is an homotopically trivial curve on the projective plane since it is continuously contractible to a point.

Examples of initial conditions that are expected to converge to discrete analogues of homotopicaly nontrivial curves in $\mathbb{R}P^2$ are

$$\phi(k) = \frac{(k-1)\pi}{N}, \quad \theta(k) = \frac{\pi}{2}, \quad s(k) = \frac{3}{\sqrt{6}};$$
 (4.11)

$$\phi(k) = \frac{(k-1)\pi}{N}, \quad \theta(k) = \frac{\pi}{2} + \frac{1}{5}\sin\frac{2\pi(k-1)}{N}, \quad s(k) = -\frac{3}{\sqrt{6}} + \frac{1}{5}\sin\frac{2\pi(k-1)}{N}; \tag{4.12}$$

k = 1, ..., N. The corresponding Q(k), and y(k) are obtained via (3.18), (3.11)-(3.14), (3.10). Figure 1(b) depicts the vectors \hat{n} of the curve defined in (4.11). The first discretizes a curve on the 2-sphere that connects antipodal points and cannot be continuously contracted to a point. In (4.12) we add a deformation, and vary the radius s.

To verify the approach to near uniaxial Q-tensors at all sites k of \overline{G} or G, we obtain Q(k) at each time t from the numerically computed y(k) at time t using the inverse of the linear transformation defined by (3.11)-(3.14), and (3.10). We further compute the eigenvalues and eigenvectors of Q(k) used in the polar representation (3.2) of Q(k), and the quantities

$$s(k) = 2\lambda_1(k) + \lambda_2(k), \quad r(k) = 2\lambda_2(k) + \lambda_1(k),$$
 (4.13)

where $\lambda_1(k) \ge \lambda_2(k) \ge \lambda_3(k)$ are the eigenvalues of Q(k) at each time. The normalized eigenvector that corresponds to $\lambda_1(k)$ is denoted by **n**, and the notation

$$\mathbf{n}(k) = [n_1(k), n_2(k), n_2(k)], \tag{4.14}$$

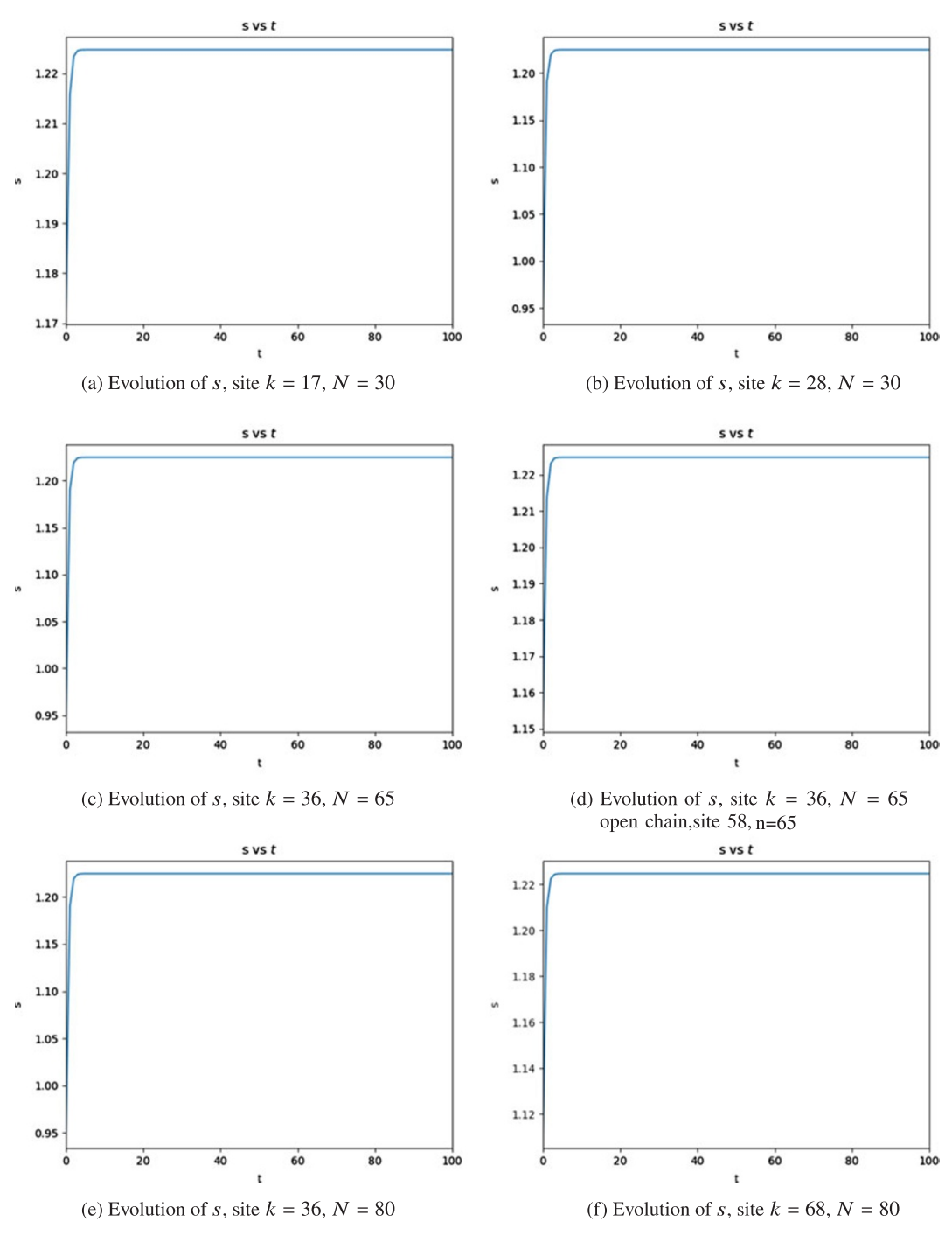


Figure 2. s v.s. t for open chains with N = 30, 65, 80, L = 0.01, see (4.13) for definition of s. Geometry A, boundary conditions (4.8), $\hat{n}(L)$, $\hat{n}(R)$ as in (3.24) with $\theta = \pi/2$, $\phi = 0$, and $\theta = \pi/2 - 0.5$, $\phi = 0.5$ respectively; initial condition as in (4.9). Parameter values $b^2 = \sqrt{6}$, $a^2 = \frac{1}{2}$, $c^2 = \frac{2}{3}$, $x_- = -\frac{1}{\sqrt{6}}$. (a) Evolution of s, site k = 17, N = 30. (b) Evolution of s, site k = 28, N = 30. (c) Evolution of s, site k = 36, N = 65. (d) Evolution of s, site k = 36, N = 65 open chain, site 58, n=65. (e) Evolution of s, site k = 36, N = 80. (f) Evolution of s, site k = 68, N = 80.

Table 1. r_{max} , s_{max} at time t for an open chain of N=65 sites, L=0.001. r_{max} , s_{max} are numbers that satisfy $|r(k)| \le r_{max}$, $s(k) \ge s_{max}$ for all $k \in \{1, ..., N\}$ at time t, see (4.13). Geometry A, boundary conditions (4.8), $\hat{n}(L)$, $\hat{n}(R)$ as in (3.24) with $\theta = \pi/2$, $\phi = 0$, and $\theta = \pi/2 - 0.5$, $\phi = 0.5$ respectively; initial condition as in (4.9). Parameter values $b^2 = \sqrt{6}$, $a^2 = \frac{1}{2}$, $c^2 = \frac{2}{3}$, $x_- = -\frac{1}{\sqrt{6}}$

t	r _{max}	Smin
0.0	1.4×10^{-1}	0.943
1.0	1.0×10^{-2}	1.190
2.0	5.8×10^{-4}	1.219
400	1.3×10^{-6}	1.225

for its components. The dependence on time is not explicit in this notation. The eigenvalues should satisfy strict inequalities in the vicinity of Σ_{-}^{3} .

4.2. Numerical observations: summary

The main observations after several integrations of the gradient flow (4.1) are the following:

- (i) All initial conditions for geometries A, and B lead to trajectories for which the Q-tensor becomes near-uniaxial after a few time units, with s, r converging to values in the vicinity of $s = -3x_-$, r = 0. The velocity of approach to near-uniaxial states is not seen to depend significantly on the number of sites N.
- (ii) All initial conditions for geometries A, and B lead to an equilibrium configuration. This occurs at a time scale that is much longer than the time scale of approach to near-uniaxial *Q*-tensors. The time to approach the equilibrium depends on the number of sites *N* and the initial condition.
- (iii) In the case of the closed chain, geometry B, we see two attracting asymptotic states, the constant state, and a state that connects two antipodal points that lie on a plane. The constant state is homotopicaly trivial and is the global minimum of the energy. The second state is a discretization of a homotopicaly non-trivial curve, similar to Figure 1(b). Multiple (at least two) stable equilibria are also observed for geometry A with some special boundary conditions. These equilibria are discrete analogues of non-homotopic curves on the projective plane and may occur under more general boundary conditions.

In what follows we describe in more detail some of numerical experiments with geometries A and B. The results below are typical a larger set of experiments performed.

4.3. Geometry A: open chain

We consider the evolution of the open chain system of (4.1) with boundary conditions y_L , y_R as in (4.8), and \hat{n} as in (3.24) with $\theta = \pi/2$, $\phi = 0$, and $\theta = \pi/2 - 0.5$, $\phi = 0.5$ respectively. Also $x_- = -1/\sqrt{6}$. The initial condition is obtained from (4.9).

The rapid approach to a near uniaxial Q-tensor is seen over a range of coupling constants $0.01 \le L \le 0.2$. Table 1 shows results using N = 65, and L = 0.01. The value of r_{max} at t = 0 indicates the departure from uniaxiality at the interior sites. The time scale of approach to near-axisymmetric tensors indicated of a few units is typical of what we saw in all numerical experiments with geometries A and B and $30 \le N \le 85$. The parameter s similarly approaches the value $s \approx 1.22$ at all sites, as expected from $s = -3x_- = \frac{3}{\sqrt{6}} \approx 1.2247$ for the radius of the critical manifold of f_B .

In Figure 2, we consider the same initial and boundary conditions with L=0.01 and three values of N=30, 65, 80. The initial conditions are obtained from the boundary values and (4.9). The plots show that the parameter s reaches the same approximate asymptotic value $s \approx 1.22$ indicating that the Q-tensor is uniaxial. The dependence of the asymptotic values of s on the site is not significant. The time taken to reach the near-uniaxial state is $t \approx 5$ for the three chains considered.

The approach to equilibrium in these experiments is indicated in Figure 3 where we show the evolution of the first component $\hat{n}_1(k)$ of the normalized eigenvector of the largest eigenvalue of Q(k) at

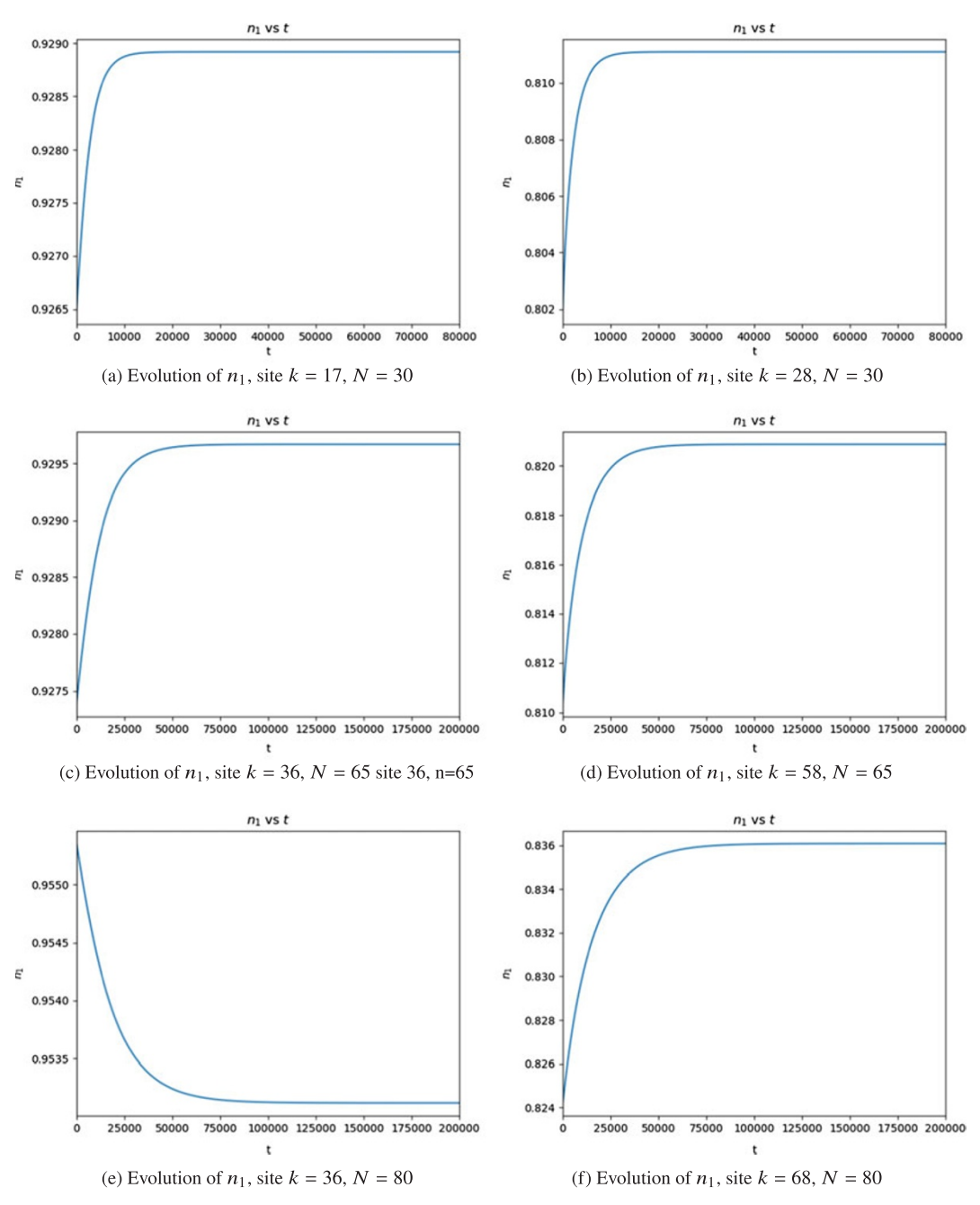


Figure 3. n_1 v.s. t for open chains of N=30, 65, 80 sites, L=0.01, see (4.14) for definition of n_1 . Geometry A, boundary and initial conditions, and parameter values as in Figure 2. (a) Evolution of n_1 , site k=17, N=30. (b) Evolution of n_1 , site k=28, N=30. (c) Evolution of n_1 , site k=36, N=65 site 36, N=65. (d) Evolution of n_1 , site k=58, N=65. (e) Evolution of n_1 , site k=36, N=80. (f) Evolution of n_1 , site k=68, N=80.



Figure 4. Numerical asymptotic (equilibrium) spatial configurations, open chain experiments of Figures 2, 3. Spatial configurations shown at times t = 80,000, (a), N = 30, and t = 200,000 for (b), (c), N = 65, 80 sites respectively

some representative sites $k \in \{1, ..., N\}$. In all the plots we see an initial rapid increase or decrease in the value of n_1 followed by a slow approach to the asymptotic value. For the case of N = 30, we show the behaviour at sites k = 17 and k = 28. The value of n_1 differs slightly between the two: at site 17, the asymptotic values is $n_1 \approx 0.9289$, while at site 28, the asymptotic $n_1 \approx 0.810$. The different values reflect the spatial pattern of the equilibrium state, and its dependence on the boundary condition. Similar time evolution patterns are observed for systems with N = 65 and N = 80 sites, see Figure 3. Figure 4 shows the spatial asymptotic spatial configurations for the N = 30, 65, 80 chains.

Figure 5 shows the evolution from initial condition

$$y(k) = -\frac{k}{N+1}(y_R - y_L), \quad k = 1, \dots, N.$$
 (4.15)

This configuration is expected to be further from the equilibrium, and the time to the reach the asymptotic values of the $\hat{n}(k)$ is longer than the time of Figure 3. The time scale is however comparable. Figure 3, 5 indicate that the approach to equilibrium is achieved at a much slower rate, e.g. a time

scale of $t \approx 10^5$. Moreover the time to equilibrium increases with the number of sites.

We also see examples of boundary conditions that lead to at least two stable equilibria. An example is shown in Figure 6 where we see two different equilibrium states for uniaxial boundary conditions of the form (3.19) with $\phi_L = 0$, $\theta_L = \pi/2$; $\phi_R = \pi/2$, $\theta_R = \pi/2$, i.e. the directors at the two ends are perpendicular. We may expect the existence of equilibria where the interior directions interpolate between the two perpendicular directions at the two edges by rotating in opposite directions. To see these two equilibria we use initial conditions are two different small perturbations of (4.9).

In the asymptotic state shown in Figure 6(a) we used initial condition (4.9), perturbed by adding 0.1 to all $y_i(k)$, i = 1, ..., 6, at site k = 1. We show the vector \mathbf{n} at the interior sites k = 1, ..., N, N = 65, at time t = 100,000. The vector \mathbf{n} at different sites is on the same plane, and we indicate the angles ϕ at sites 1, 32, and 65 (0.02, 0.72 and 1.55 respectively in radians). (The angle θ is approximately $\pi/2$ in all the sites.) In the asymptotic state shown in Figure 6(b), we used initial condition (4.9), perturbed by adding -0.07 to all $y_i(k = 65)$, i = 1, ..., 6 at site k = 65. We show the vector \mathbf{n} at the interior sites k = 1, ..., N, N = 65, at time t = 100,000. Again, the vector \mathbf{n} at different sites is on the same plane, and we indicate the angles ϕ angles sites 1, 32, and 65 (1.55, 0.86, 0.02, respectively, in radians). We see that the two configurations are different, e.g. the angle difference at k = 32 is 1.47, close to $\pi/2 \approx 1.57$. Each configuration also exhibits different helicity as the direction rotates in opposite directions as we move from the left to the right end of the chain, which are

The above solutions are discrete analogues of curves γ_1 , γ_2 on the unit sphere S^2 that connect each of the unit vectors \mathbf{m} , $-\mathbf{m}$ to a third unit vector \mathbf{p} , $\mathbf{p} \perp \mathbf{m}$ and also belong to the plane of \mathbf{m} , \mathbf{p} . The two curves define curves $\tilde{\gamma}_1$, $\tilde{\gamma}_2$ on $\mathbb{R}P^2$ that are not homotopic since a homotopy of $\tilde{\gamma}_1$ to $\tilde{\gamma}_2$ would produce a homotopy of the homotopically nontrivial closed curve $\tilde{\gamma}$ obtained from concatenating γ_1 and γ_2 and projecting to $\mathbb{R}P^2$ to the homotopically trivial curve from $\{\mathbf{m}, -\mathbf{m}\}$ to $\{\mathbf{p}, -\mathbf{p}\}$ and then back to $\{\mathbf{m}, -\mathbf{m}\}$. Thus the two solutions seen are discretizations of two non-homotopic curves on $\mathbb{R}P^2$.

Analogous curves γ_1 , γ_2 on S^2 can be obtained by connecting unit vectors **m** and $-\mathbf{m}$ to a third unit vector **p** that is not perpendicular to **m**. The two curves are again chosen to lie to the plane of **m**, **p**,

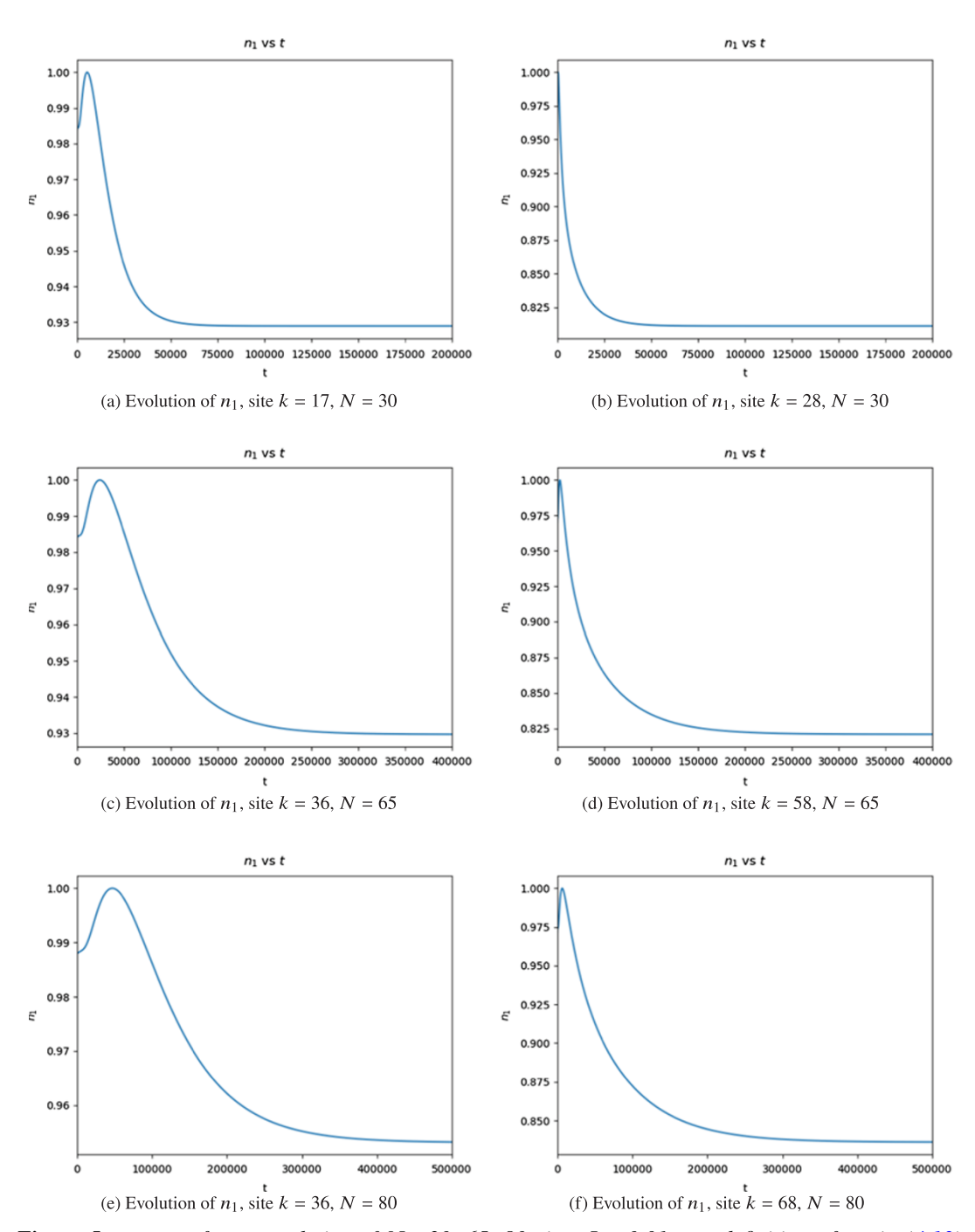


Figure 5. n_1 v.s. t for open chains of N=30, 65, 80 sites, L=0.01, see definition of n_1 in (4.13). Geometry A, boundary conditions and parameter values as in Figures 2, 3. Initial conditions are obtained from (4.15), different from those of Figures 2, 3. (a) Evolution of n_1 , site k=17, N=30. (b) Evolution of n_1 , site k=28, N=30. (c) Evolution of n_1 , site k=36, N=65. (d) Evolution of n_1 , site k=36, N=80.

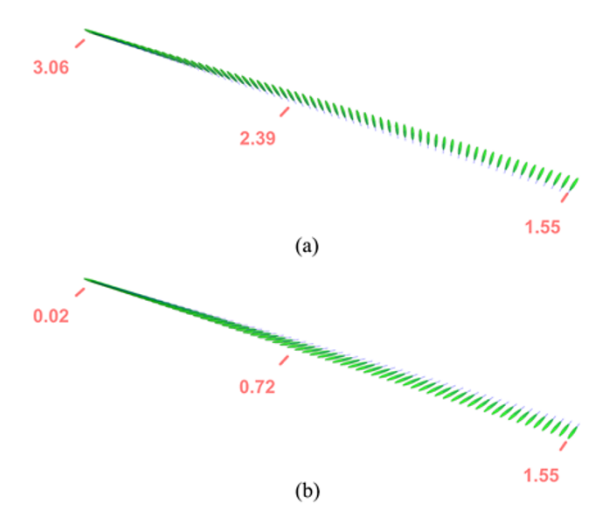


Figure 6. Evidence for bistability for a uniaxial boundary condition where the directions at the two boundary points are perpendicular, open chain geometry A, N = 65 sites. Boundary conditions for (a), (b) given by Q-tensor of (3.19), with $\phi_L = \pi/2$, $\theta_L = \pi/2$; $\phi_R = 0$, $\theta_R = \pi/2$ for left and right boundaries respectively. Initial conditions for (a), (b) two are different perturbations of (4.9) at the leftmost interior site k = 1. Figures (a), (b) show the corresponding vector \mathbf{n} at t = 100000. In both cases lies on on the same plane at all sites and we show values (in radians) of direction angles at sites k = 1, 32, 65. The angle difference at k = 32 is 1.47, close to $\pi/2 \approx 1.57$, thus the configurations of (a), (b) are different, and have opposite helicity.

and similarly define curves $\tilde{\gamma}_1$, $\tilde{\gamma}_2$ on $\mathbb{R}P^2$ that are not homotopic. The curves γ_1 , γ_2 would now have different lengths. Their discretized analogues would interpolate between different endpoint angles, and are expected to have different energies and basins of attraction.

4.4. Geometry B: homotopicaly trivial and nontrivial equilibria

In periodic chains we observe that the gradient system has at least two attracting equilibria, corresponding to the two homotopy classes of the projective plane. In all integrations we see a fast approach to near-uniaxial *Q*-tensors, and a slower approach to the equilibria. The fast and slow time scales are comparable to those seen in the open chain examples.

An example of convergence to the homotopically trivial constant state is shown in Figure 7, where we see the evolution of $\hat{n}_2(k)$ for some sites k. Components $n_1(k)$, $n_3(k)$ tend to 0 in all the sites k. We use L = 0.01, N = 30, 65, 80, and the initial condition (4.10). Figure 7 shows the evolution of n_2 . The asymptotic state is constant. The initial and asymptotic states are shown in Figure 8. Figure 7 shows that the time of convergence increases with the size of the chain N. The convergence to the equilibrium is comparable but faster than the convergence to the equilibrium of Figure 3 for the open chain.

The homotopicaly trivial equilibrium is the state where the Q-tensor is uniaxial and takes the same value at all sites. This state corresponds to the global minimum of the energy since it minimizes both parts of the Landau–de Gennes energy.

We have also seen convergence to a discrete analogue of a homotopically non-trivial state. In Figures 9, 10 we show results from integration with the initial condition of (4.12), using L = 0.01 and chain sizes N = 30, 65, 80. The convergence to near-uniaxial tensors occurs rapidly as in the previous cases and is not shown. Figure 9 shows the slower convergence of n_1 at two sites for N = 30, 65, 80. Figure 10 shows the evolution of the vectors \hat{n} after their rapid approach to projective plane defined by $s = -3x_-$, r = 0. The time scale is comparable to that of the previous examples. The main observation is that the vectors $\hat{n}(k)$ belong to a plane, for all $k \in \{1, ..., N\}$. This state is stable. The system may have additional

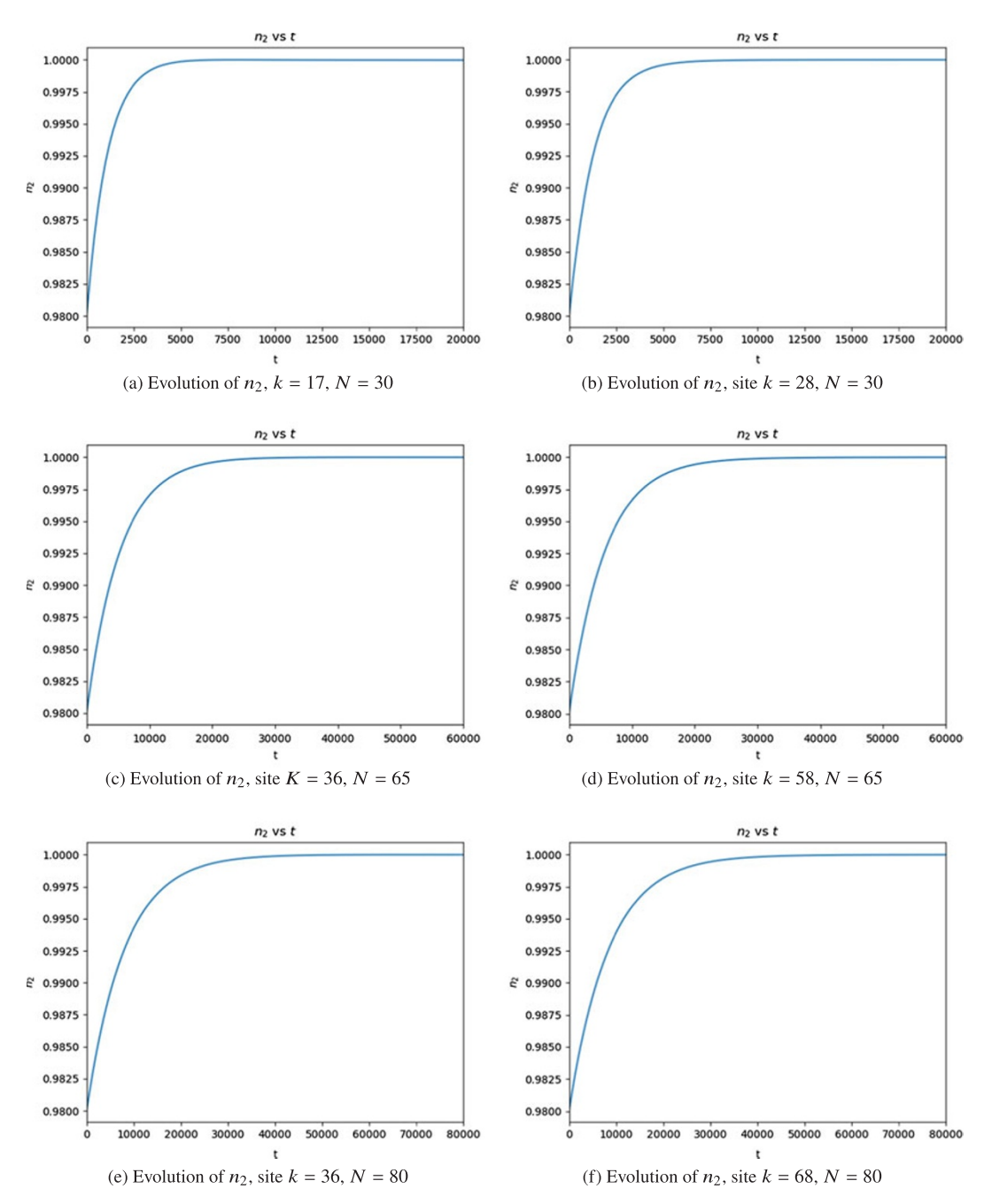


Figure 7. n_2 v.s. t for periodic chains with N=30, 65, 80 sites, L=0.01, definition of n_2 in (4.14). Geometry B, initial condition of (4.10) discretizes homotopically trivial curve on projective plane. Parameter values $b^2 = \sqrt{6}$, $a^2 = \frac{1}{2}$, $c^2 = \frac{2}{3}$, $x_- = -\frac{1}{\sqrt{6}}$. (a) Evolution of n_2 , k=17, N=30. (b) Evolution of n_2 , site k=28, N=30. (c) Evolution of n_2 , site k=36, N=65. (e) Evolution of n_2 , site k=36, N=80. (f) Evolution of n_2 , site k=68, N=80

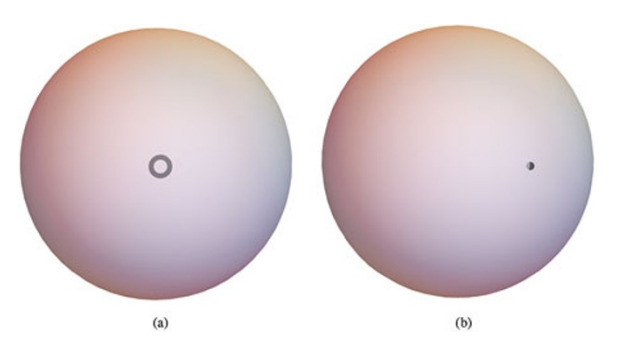


Figure 8. Normalized vectors $\mathbf{n}(k)$, $k = 1, \dots N$, N = 65, at two different times for homotopicaly trivial configuration, experiment of Figure 7, N = 65, see (4.14). (a) Initial configuration of vectors $\mathbf{n}(k)$, as in (4.10). (b) Numerical asymptotic configuration of vectors $\mathbf{n}(k)$ (t = 200000). The vectors are visualized on the 2-sphere, (a), (b) use different perspectives.

equilibria corresponding to nontrivial homotopy classes of the circle. The existence and stability of additional equilibria will be examined elsewhere.

5. Discussion

We have considered a discrete version of the Landau–de Gennes theory in graphs and lattices without boundary in the regime of small intersite coupling L. The main theoretical results are necessary and sufficient conditions for continuation of equilibria of the decoupled system and the presence equivariance of the reduced or bifurcation equations. The proof uses the strategy of [26] that also implies the existence of a normally hyperbolic invariant manifold of the gradient flow of the Landau–de Gennes that is parametrized by the uniaxial Q-tensors. The theory makes use of the symmetry of the on-site energy under rotations, this structure and related results should be relevant to more general discrete parabolic multicomponent systems with symmetries under Lie group actions.

We also report results from numerical integration of the Landau–de Gennes gradient flow for two simple one-dimensional geometries, an open chain, and a periodic chain. We observe rapid approach to a near-uniaxial state, and a slower convergence to the equilibrium. The fast scale is independent of the size of the chain while the slow scale increases with the size of the chain. In closed chains we see at least two stable equilibria that are discrete analogues of the two homotopy classes of the projective plane. We also see bistability in the open chain, under boundary conditions of perpendicular directors at the two endpoints.

The equilibria seen here are uniaxial Q-tensors with directions that lie on the same plane at all sites. Connections with the theory for 2×2 Q-tensors [25] should be examined further. We expect additional equilibria of periodic and open chains that correspond to homotopy classes of S^1 with higher rotation number. These solutions are expected from the theory of discrete vortices in the discrete Schrödinger equation [29]. Their stability in the 2×2 and 3×3 Q-tensor theories could be studied further. Further work will address similar effects in more general one-dimensional geometries, e.g. discrete analogues of some graphs, where we may see some discrete analogues of dislocations. One of our future goals is to examine higher dimensional geometries and domains such as the disc on the plane. Also of interest are phenomena of front propagation in discrete Landau–de Gennes equation and related parabolic systems, see e.g. [7]. In the Landau–de Gennes system these are fronts connecting the isotropic and nematic states, where Q = 0, and $Q \in \Sigma_-^3$, respectively. The nematic region is expected to expand since the isotropic state is unstable.

As mentioned in section 2, the discrete theory is relevant to numerical simulations of continuous models and experimental studies. The calibration of the parameters of the discrete model is discussed in [8, 22, 32]. One of the main observable consequences of the theory is the geometrical shape of

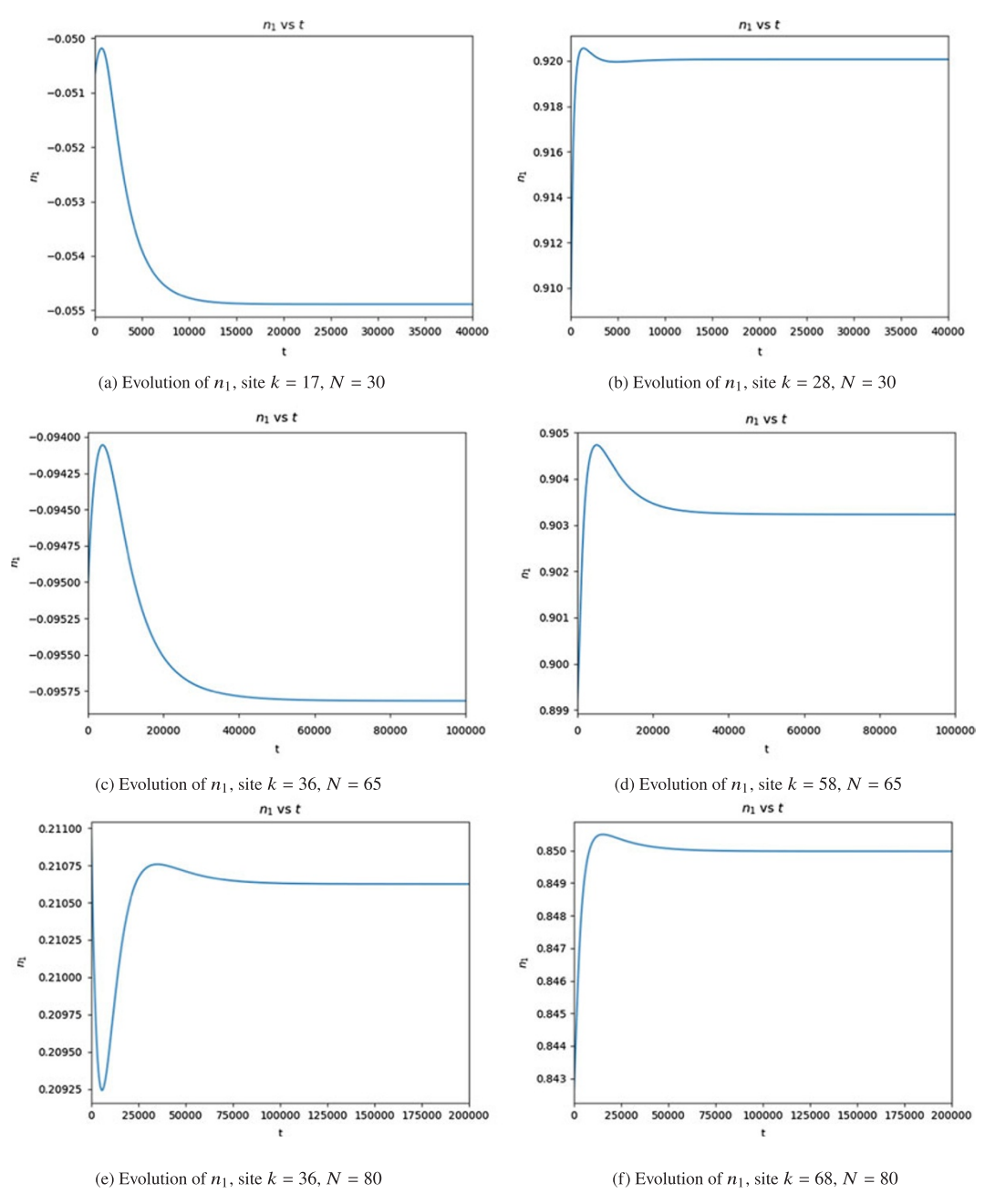


Figure 9. n_I v.s. t for periodic chains with N=30, 65, 80 sites, L=0.01. Initial condition of (4.12) discretizes homotopically non-trivial curve on projective plane. Parameter values $b^2 = \sqrt{6}$, $a^2 = \frac{1}{2}$, $c^2 = \frac{2}{3}$, $x_- = -\frac{1}{\sqrt{6}}$. (a) Evolution of n_I , site k=17, N=30. (b) Evolution of n_I , site k=28, N=30. (c) Evolution of n_I , site k=36, N=65. (d) Evolution of n_I , site k=58, N=65. (e) Evolution of n_I , site k=36, N=80. (f) Evolution of n_I , site k=68, N=80.

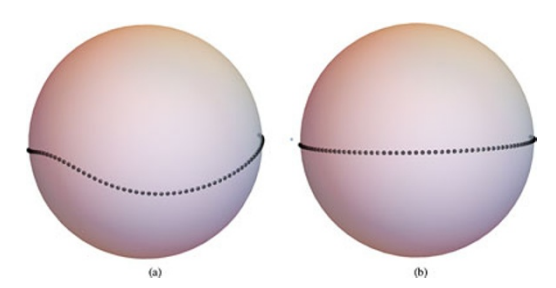


Figure 10. Normalized vectors $\mathbf{n}(k)$, k = 1, ..., N, N = 65, at two different times for homotopicaly nontrivial configuration, experiment of Figure 9, N = 65, initial configuration as in (4.12). (a) Configuration of vectors $\mathbf{n}(k)$ at t = 1000. (b) Numerical asymptotic configuration of vectors $\mathbf{n}(k)$ (t = 200000).

the nematic field, detected optically. Qualitative features such as dislocations and their positions seen in two-dimensional simulations are therefore observable. The present study indicates multistabilty in simple geometries that can also be detected optically. A possible quantitative result is the time to reach the equilibrium, and its dependence on the coupling constant, boundary conditions, and the size of the domain.

Data availability statement. All numerical can be made available upon request.

Acknowledgments. We acknowledge helpful discussions with Adrian Reyes and Carlos Garcia Azpeitia.

Author contributions. Conceptualization: P.P.; G.R.V. Methodology: P.P.; G.R.V. Formal Analysis: P.P.; G.R.V. Software: P.P.; G.R.V. Visualization: G.R.V. Writing – original draft: P.P.; G.R.V. Writing – review & editing: P.P.; G.R.V. All authors approved the final submitted draft.

Funding statement. This research was supported by grants DGAPA-UNAM PAPIIT IG100522, and IN103725, SECIHTI CF-2023-I-65, and SECHITI Estancias Posdoctorales por México.

Competing interests. None.

Ethical standards. The research meets all ethical guidelines, including adherence to the legal requirements of the study country.

References

- [1] Assanto G and Karpierz M (2009) Nematicons: Self-localized beams in nematic liquid crystals, *Liquid Crystals* 36, 1161–1172.
- [2] Aubry S and Daeron PYL (1983) The discrete Frenkel-Kontorova model and its extensions: I. Exact results for the ground states, *Physica D* 8, 381–422.
- [3] **Bates PW, Lu K and Zheng C** (1998) Existence and persistence of invariant manifolds for semiflows in Banach space, *Memoirs of the American Mathematical Society* **645**, 1–129.
- [4] Berger P and Bounemoura A (2013) A geometrical proof of the persistence of normally hyperbolic submanifolds, Dynamical Systems 28, 567–581.
- [5] Buffoni B and Tolland J (2003) Analytic Theory of Global Bifurcation, Princeton: Princeton University Press.
- [6] Burns K and Gidea M (2005) Differential Geometry and Topology, Boca Raton: Chapman and Hall/CRC.
- [7] Caputo JG, Cruz G and Panayotaros P (2015) Bistable reaction-diffusion on a network, *Journal of Physics A: Mathematical and Theoretical* **48**(7), 075102. doi:10.1088/1751-8113/48/7/075102.
- [8] Davis TA and Gartland JEC (1998) Finite element analysis of the Landau-de Gennes minimization problem for liquid crystals, SIAM Journal on Numerical Analysis 35, 336–362.
- [9] De Gennes PD and Prost J (1974) The Physics of Liquid Crystals, Oxford: Clarendon Press.
- [10] Eldering J (2013) Normally Hyperbolic Invariant Manifolds: The Noncompact Case, Paris: Atlantis Press.
- [11] Fenichel N (1971/1972) Persistence and smoothness of invariant manifolds for flows, *Indiana University Mathematics Journal* 21, 193–226.
- [12] **Forrest MG, Wang Q and Zhou H** (2000) Exact banded patterns from a Doi-Marruci-Greco model of nematic liquid crustal polymers, *Physical Review E* **61**, 6655–6662.
- [13] Frank FC (1958) On the theory of liquid crystals, Discussions of the Faraday Society 15, 1.

- [14] Gartland JEC (2021) Electric-field-induced instabilities in nematic liquid crystals, SIAM Journal on Applied Mathematics. 81, 304–334.
- [15] Hirsch MW, CC Pugh and M Shub. 1977. Invariant Manifolds. Lecture Notes in Mathematics, 583, Springer, Berlin.
- [16] Kolář I, Michor PW and Slovák J (1993) Natural Operations in Differential geometry, Berlin: Springer.
- [17] Lee JM (2009) Manifolds and Differential Geometry, AMS, Providence.
- [18] Lee JM (2013) Introduction to Smooth Manifolds, New York: Springer.
- [19] MacKay RS and Aubry S (1994) Proof of existence of breathers for time-reversible or Hamiltonian networks of weakly coupled oscillators, *Nonlinearity* 7, 1623–1643.
- [20] Majumdar A (2010) Equilibrium order parameters of nematic liquid crystals in the Landau–de Gennes theory, European Journal of Applied Mechanics 21, 181–203.
- [21] Majumdar A and Zarnescu A (2010) Landau-de Gennes theory for nematic liquid crystals: the Oseen-Frank limit and beyond, Archive for Rational Mechanics and Analysis 196, 227–280.
- [22] Martinez-Gonzalez JA, Li X, Sadati M, Zhou Y, Zhang R, Nealey PF and de Pablo JJ (2017) Directed self-assembly of liquid crystalline blue-phases into ideal single-crystals, *Nature Communications* 8, 15854.
- [23] Michor PW (2008) Topics in Differential Geometry, AMS, Providence.
- [24] Mkaddem S and Gartland EC (2000) Fine structure of defects of radial nematic droplets, *Physical Review E* 62, 6694–6705.
- [25] Panayotaros P (2022) Equilibria of a discrete Landau-de Gennes theory for nematic liquid crystals, European Physical Journal - Special Topics 231, 297–307.
- [26] Panayotaros P (2023) Stationary solutions of discrete Landau–de Gennes theory: 3 x 3 Q-tensor case, Physica D 449, 133751.
- [27] Panayotaros P and Pelinovsky DE (2008) Periodic oscillations of discrete NLS solitons in the presence of diffraction management, Nonlinearity 21, 1265–1279.
- [28] Peccianti M and Assanto G (2012) Nematicons, Phys. Rep. 516, 147–208.
- [29] Pelinovsky DE, Kevrekidis PG and Frantzeskakis DJ (2005) Persistence and stability of discrete vortices in nonlinear Schrödinger lattices, *Physica D* 212, 20–53.
- [30] Pelinovsky DE, Kevrekidis PG and Frantzeskakis DJ (2005) Stability of discrete solitons in nonlinear Schrödinger lattices, Physica D 212, 1–19.
- [31] Penati T, Sansottera M, Paleari S, Koukouloyannis V and Kevrekidis PG (2018) On the nonexistence of degenerate phase-shift solitons in a dNLS nonlocal lattice, *Physica D* 370, 1–13.
- [32] Ravnik M and Žumer S (2009) Landau-de Gennes modelling of nematic liquid crystal colloids, *Liquid Crystals* 36, 1201–1214.
- [33] Sansottera M, Danesi V, Penati T and Paleari S (2020) On the continuation of degenerate periodic orbits via normal form theory: Lower dimensional resonant tori, Communications in Nonlinear Science and Numerical Simulation 90, 105360.